Doctoral Dissertation

Study on the three-dimensional thermo-sensing system using

a computer vision

コンピュータビジョンを用いた三次元サーモセンシングシステムに関する研究

March 2014

Interdisciplinary Graduate School of Agriculture and Engineering
Department of Materials and Informatics
Course of Production Technology
University of Miyazaki

Tao Li

宮 崎 大 学 大 学 院

博 士 学 位 論 文

Study on the three-dimensional thermo-sensing system using

a computer vision

コンピュータビジョンを用いた三次元サーモセンシングシステムに関する研究

2014 年 3 月

宮崎大学大学院農学工学総合研究科

物質・情報工学専攻

李　涛

Table of Contents

CHAPTER 1: General Introduction

1.1 Background

Generally, infrared thermography is used to measure the distribution of infrared energy emitted from the surface of an object. Since a two-dimensional thermal image can be easily obtained without making contact with the object, and image processing can be easily performed by a computer, the thermography has been used in fields such as agriculture, medicine, engineering, and architecture.

In recent years, with the development of signal processing technology and devices, thermal imaging measurement technology has developed rapidly. Amid this development, small, lightweight infrared thermography devices are becoming popular, and the performance of infrared thermography, in terms of factors such as measurement resolution, accuracy, number of pixels, and measurement speed, has been improved. Application technology based on infrared thermography has also made great strides as a result of improvements in hardware. Non-destructive evaluation of buildings and metal materials is an example of such an approach. However, since images used in such evaluations are two-dimensional (2D) thermal images, quantitative information such as the area, the three-dimensional (3D) shape, and the roughness of heat source, cannot be obtained. The ability to acquire 3D location and temperature information is useful in various fields, including agriculture, medicine and industry. For example, it is useful for measuring energy budget balance of livestock in agriculture. In addition, it is also useful for restoration works of building and prediction of risk after a disaster occurs.

Temperature information can be obtained by infrared thermography. On the other hand, methods for obtaining 3D location information can be divided into contact and non-contact methods. Contact methods retrieve data by placing a probe in contact with the target object. Although high-accuracy measurement of a small region can be achieved using this method, acquiring data for a large area takes a long time. In addition, since contacting the object may

damage it, contact methods are not desirable in many fields. There are two types of non-contact methods, i.e., the passive stereo method and the active light-section method, which can obtain quantitative location information in a short time. In the stereo method, based on the positional relationship of the same points projected onto the projection plane which is capturing measurement points from different viewpoint in 3D space, 3D position information can be obtained by triangulation principle. In the light-section method, a slit laser is projected onto the measurement object and the laser streak image appearing on the surface of the object is observed by a camera. Then, luminous points on the laser streak are extracted and 3D coordinates of these points are calculated by the coordinate relationship between the pixel coordinate and the world coordinate. In order to acquire 3D shape of an object, it is necessary to scan the slit laser.

In recent years, three-dimensional measurement technology requires measurement of both 3D shape and temperature information, such as the temperature distribution and the heat radiation state of electronic devices during operation. Therefore, in the present paper, three types of image measurement systems that can detect both the 3D shape and the temperature distribution of a target object have been developed. The proposed measurement systems can measure both position and temperature information simultaneously using a single instrument. The present paper describes the measurement principles, analysis methods, and accuracy evaluation for the three systems. In addition, the validity of the proposed methods and the convenience of the systems were investigated.

Based on previous studies on the quantification of object shape, the proposed measurement systems were established by combining thermography with 3D surface measurement technology.

1.2 Past studies

1.2.1 Research paper on infrared thermography

In recent years, with the development of signal processing technology and devices, infrared thermography can easily capture 2D thermal image without making contact with the object with a high accuracy, and can detect a small temperature change of the non-steady. Therefore, application technology based on infrared thermography has been widely used in various fields such as medical and engineering. A large number of studies on non-destructive evaluation of concrete structures and metal materials have been reported [1]-[3]. For example, the author [1] described about thermo-elastic stress measurement method by measuring the variation of the stress acting on the object based on a small temperature variation of the object caused by the elastic deformation. However, since these images used in such evaluations are tow-dimensional thermal images, and quantitative information such as the three-dimensional shape, the area and the 3D temperature distribution of an object, cannot be obtained.

In order to obtain the quantitative information, the present paper proposed a measurement model that enables combining three-dimensional scanning technology with thermography to produce standardised 3D thermograms, so that a new base for medical applications can be provides.

1.2.2 Research paper on the quantification of object shape

Quantification technique of an object shape is widely used in the industrial production field. Specially, the technique is used for automatic position detection and automatic inspection of component shape in the production site. It is also an important technology with respect to improvement of productivity and working efficiency in the production line. Practical application has advanced to measure the machine parts and molds using the quantification technology. In recent years, application fields have spread to measure human body, character model and agricultural crops. Quantification of object shape is well studied for a long time, and many measurement methods have been proposed [4-14]. For example, the author [9] had proposed a measurement method (light section method) that a laser light sheet or dots is projected on the surface of an object, and bright lines or bright dots appeared on the surface are detected by a camera. Then, three-dimensional position information of bright lines is determined by a triangulation process based on the relationship between the pixel coordinates and the world coordinates. At last, three-dimensional shape of the object is obtained by scanning the laser. In order to acquire the shape of the entire object, it is necessary to scan the slit laser in the surface of the entire object. In the proposed method of the authors [9], since the device is non-mobile, occlusion problem will occur when measuring 3D shape of an uneven object. Quantification of the object shape by a light section method is superior in that it can be acquired with high accuracy, but there are three disadvantages such as imperfections, non-instantaneous nature and discreteness. The first disadvantage is imperfections that the shape of occluded segment cannot be acquired from a camera. The second disadvantage is non-instantaneous nature that constructing 3D shape takes a long time since it is necessary to scan the laser. The third disadvantage is discreteness since the shape data can be obtained discretely. In addition, the authors [14] proposed a new method. The same measuring object is captured using two cameras from different viewpoint, and the 3D shape of the object is reconstructed based on the extraction of feature points on the object. In this method, in order to obtain 3D position information

correctly, accuracy of detection and correspondence of feature points is very important. This measurement method has been used anciently. Although depth information can be easily obtained [14], the method is not suitable to measure the 3D shape of an object with high accuracy since measurement accuracy is lower.

In this paper, a measurement system using a light-section method is proposed. On the basis of the presented mathematical model, it is possible to detect not only the three-dimensional shape but also the temperature distribution of an object. This paper described a mapping method that can allocate temperature information to the corresponding 3D position obtained by 3D measurement technology. Effectiveness of the proposed measurement system was shown through experiment.

1.3 Summary of this paper

1.3.1 Purpose and constitution of this paper

The purpose of the present study is to develop an image measurement system that can detect not only the 3D shape of a target object but also its temperature distribution using a single instrument. The following three studies have been carried out:

 (1) Study on three-dimensional thermal image

 (2) System development using handheld 3D measuring instrument

 (3) Research on high accuracy by combing a light-section method and a magnetic sensor

This paper is organized into five Chapters. The content of each Chapter is described as follows.

In Chapter 1, general introduction was introduced. This Chapter described the structure, the purpose and the research background of the present study.

In Chapter 2, the subjacent measurement method that can obtain 3D temperature distribution of an object was introduced. Although standard infrared thermography can capture the two-dimensional temperature distribution as a thermal image without making contact with a target object, quantitative information, such as the area and shape of a heat source, cannot be obtained. In this Chapter, an image measurement device that can measure the 3D shape and the surface temperature distribution of an object simultaneously is proposed, and its principles are described. The measurement device was realized by combining thermography with a 3D shape measurement method that uses a laser (light-section method). The light-section method was performed by moving a slit laser projector attached to a uniaxial stage. Three-dimensional thermal imaging was carried out by mapping a 2D thermal image to the obtained 3D position.

The measurement device proposed in Chapter 2 cannot measure the shape of the back of a target object using the light-section method because the back of the object cannot be observed by the camera. Therefore, in Chapter 3, a measurement system composed of a portable 3D measurement instrument (Kinect sensor) and an infrared thermography device is proposed. The

measuring system was realized by mapping a thermal image obtained by thermography to 3D position information obtained by a portable 3D measurement instrument. By moving the instrument, the entire perimeter of the target object can be measured by splicing the obtained shape data automatically using the iterative closest point (ICP) algorithm. The feasibility of the measurement device is demonstrated experimentally by measuring the temperature distribution of a cylindrical target object.

Although the measurement method proposed in Chapter 3 enabled measurement of the shape of the entire object, the measurement accuracy, which depends on the performance of the 3D measurement instrument (Kinect sensor), was poor. However, higher measurement accuracy sometimes is required, depending on the nature of the target object. In Chapter 4, in order to improve the measurement accuracy, a measurement system that was composed of a laser-projection unit, an image-capture unit (CCD camera and thermography) and magnetic sensors was introduced. Here, the laser-projection unit and the image-capture unit can be moved freely by mounting magnetic sensors on them, thus allowing real-time detection. Therefore, measurement of 3D temperature distribution was realized by maintaining the proper angle between the laser-projection unit and the image-capture unit.

Chapter 5 summarizes the paper.

1.3.2 Feature of the present study

In recent years, researches on the three-dimensional measurement of an object shape, such as, measurement of the tunnel wall, the sewer pipe and the road, have been reported in great numbers. The obtained point cloud data contains only the position information. However, it is required to measure not only the three-dimensional shape but also temperature distribution of a target object in many cases. Especially, acquiring 3D thermal data is useful for restoration work of building and prediction of risk after a disaster occurs. After the Fukushima Daiichi nuclear disaster, temperature information obtained by the thermograph is required more and more in many fields. Therefore, In order to respond to the demand of society, the 3D measurement technology proposed in the present study is different from conventional three-dimensional measurement technology. The measurement systems that can detect not only three-dimensional shape of an object but also its surface temperature distribution were proposed. Application technology based on infrared thermography can make great strides in biological and medical fields by acquiring the 3D temperature distribution.

In this paper, measurement of 3D surface temperature distribution of a target object was realized using one measuring instrument.

CHAPTER 2: Study on three-dimensional thermal image

2.1 Introduction

In recent years, a diverse array of image measurement techniques has been rapidly developed as a result of the evolution of signal processing technology and device development. In particular, techniques involving infrared thermography have improved greatly. Infrared thermography can capture the 2D temperature distribution as a thermal image and so has been used in various fields, such as medicine, biology, and industry. For example, in medicine and biology, in order to capture inflammation and pain of the knee, infrared thermography is used to measure the effectiveness of blood circulation accelerators, the effectiveness of drugs, the correlation between temperature increase and pain, and the temperature distribution of inflammation in the knee [15][16]. However, since the images obtained by infrared thermography are two-dimensional thermal images, quantitative information about the position and temperature distribution cannot be obtained.

   Therefore, in this Chapter, an image measurement device that can simultaneously measure the 3D shape and the surface temperature distribution of an object is proposed. The proposed device is based on the combination of infrared thermography and a 3D shape measurement method (light-section method). This Chapter describes the principle of the measurement device and the analysis method. Specifically, the light-section method was realized by moving a slit laser projector attached to a uniaxial stage. The slit laser is projected on the target object and the laser streak appeared on the surface of the object is captured by CCD camera and thermography simultaneously. Then 3D coordinates of points on the slit laser are calculated by a triangulation process. Finally, measurement of 3D thermogram is realized by mapping the temperature data to the corresponding 3D position. Here, in order to calculate the 3D coordinates of points on the slit laser, it is necessary to calibrate the camera and the thermography device in advance. Calibration methods for the camera and the thermography device are proposed in this Chapter.

2.2 Configuration of measurement system

The measurement system is shown in Fig.2-1. This system is established using a three-dimensional shape measurement system and a thermography. The three-dimensional shape measurement system is composed of a CCD camera and a laser projector. Three-dimensional coordinates of points on a target object can be calculated by active triangulation process. The 3D surface shape of an object can be obtained by scanning the slit laser using the light-section method [8]-[9]. Then the corresponding temperature data obtained by the thermography is allocated to the reconstructed surface shape of the object on a computer.

Specifically, the laser projector equipped on a uniaxial stage is projected on the surface of an object. The laser streak appeared on the surface of the object is recorded by the CCD camera and the thermography simultaneously, and three-dimensional coordinates of points on the target object are calculated by analyzing the laser streak. The thermal data obtained by the thermograph is allocated to the corresponding three-dimensional position using conversion matrix as equation (5). In order to measure global surface shape of a target object, it is necessary to scan the slit laser. Since the laser project is equipped on the uniaxial stage and the uniaxial stage is controlled by computer, the global surface shape of the target object can be measured by moving the slit laser at 1 mm interval. Here, calibration of camera and thermography is carried out in advance. Calibration is an important task in three-dimensional measurement since it can determine three-dimensional position of the slit laser and allocate the corresponding temperature data to the reconstructed surface shape of the target object. Generally, calibration process is complicated and is not unified in three-dimensional measurement system. In this proposed system, since relationship between the coordinates, such as between the pixel coordinate and the world coordinate, between the world coordinate and the thermography coordinate, influences the allocation accuracy, they have to be determined precisely on the calibration process. The suitable calibration method for the CCD camera and the thermography is proposed in this Chapter.
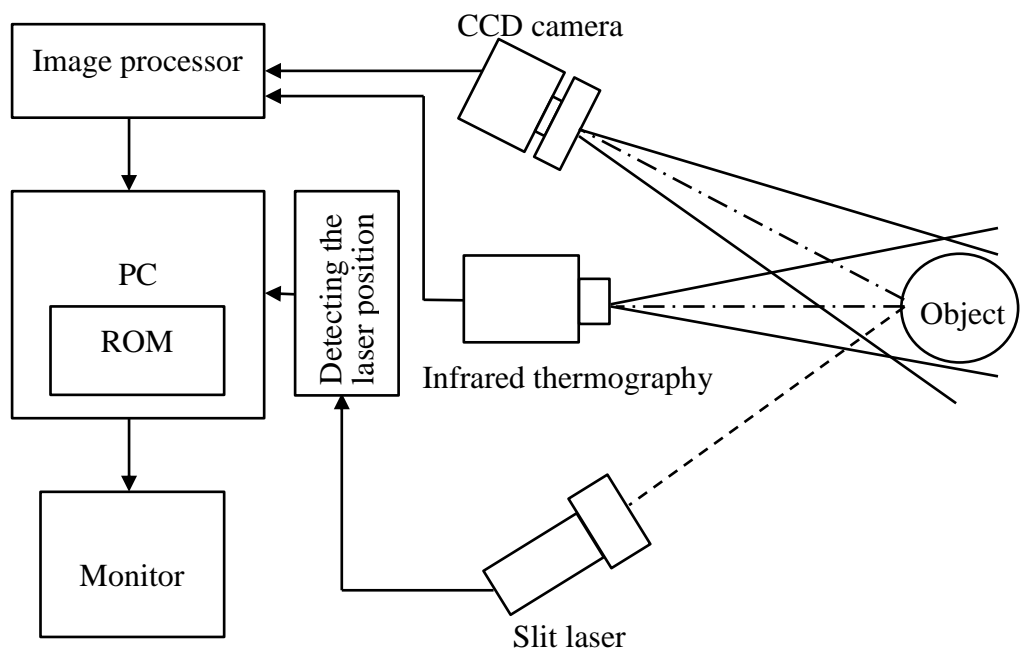
Fig.2-1 Measurement system.

2.3 Measurement principle

2.3.1 Method of image processing

In order to measure the surface shape of an object, it is necessary to extract laser emission line appeared on the surface of the object. In this study, the laser emission line is extracted by binary image processing method. The binarization is a process for converting the binary image that is either black or white as a boundary in value (threshold). Here, the pixel in the binary image includes color information or density information. Binary image processing occupies a unique position in the computer image processing. In order to analyze the features of the image, binarization processing is often used to cut out an object from an image, and to separate the background and shape in many cases. Binarization of the image is performed by threshold processing as follows.

$$f_t(i,j) = \begin{cases} 1; f(i,j) \geq t \\ 0; f(i,j) < t \end{cases} \tag{1}$$

Generally, the portion of value 1 in the binary image $f_t(i,j)$ is the target shape, and the portion of value 0 is background. There are two methods to determine the threshold t. It is p-tile method and mode method. Fig.2-2 shows an example of binarization processing (Door mirror, Honda Lock Co., Ltd.).
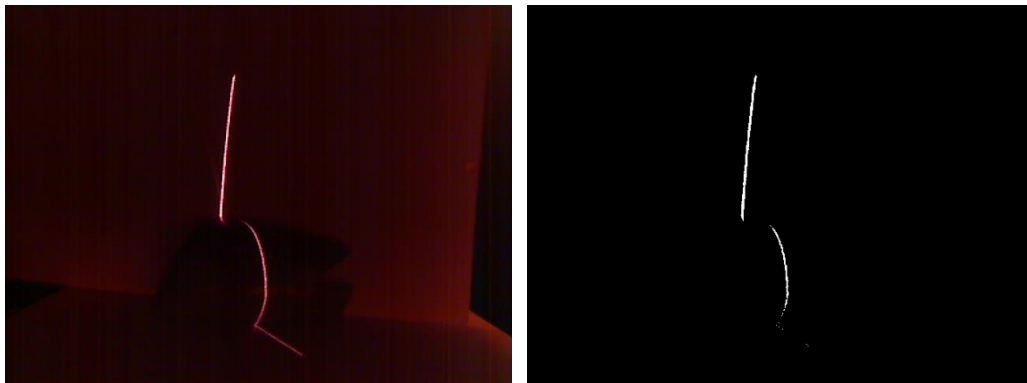

Fig.2-2 Example of threshold processing.

2.3.2 Camera calibration

If you move a camera when taking pictures with a camera, the pictures will vary by the position and posture of the camera. In addition, even if the position and posture of the camera is the same, the images also change as the camera and lens are different. Conversely, it may be known how to take the image from any location and orientation by analyzing the captured pictures. Thus, it is called camera calibration which estimates the characteristic and the position posture of the camera from the captured images. Fig.2-3 shows the relationship between the pixel coordinate and the world coordinate. As shown in Fig.2-3, the distance from camera focus to projection plane is shown as focal distance f. The relationship between the pixel coordinate (u, v) and the world coordinate (x, y, z) is formulated as follows [4][17]-[19].

$$s \begin{bmatrix} u \\ v \\ 1 \end{bmatrix} = \begin{bmatrix} k_{11} & k_{12} & k_{13} & k_{14} \\ k_{21} & k_{22} & k_{23} & k_{24} \\ k_{31} & k_{32} & k_{33} & 1 \end{bmatrix} \cdot \begin{bmatrix} x \\ y \\ z \\ 1 \end{bmatrix} \tag{2}$$

Where k_{11} to k_{33} are parameters that consider the rotation, scale and displacement between pixel coordinates and world coordinates. These parameters can be determined by inputting some corresponding positions between pixel coordinates and world coordinates. In this system, a calibration block is used to match the coordinates between pixel coordinates and world coordinates. The parameters k_{11} to k_{33} are calculated by inputting over 6 corresponding point to equation (2). Since the slit laser moves along the uniaxial stage at 1mm interval, the z coordinate is indicated for the amount of movements of the uniaxial stage. The equation (2) can be written as follows.

$$\begin{bmatrix} x \\ y \end{bmatrix} = \begin{bmatrix} k_{31}u - k_{11} & k_{32}u - k_{12} \\ k_{31}v - k_{21} & k_{32}v - k_{22} \end{bmatrix}^{-1} \cdot \begin{bmatrix} (k_{14} - u) - (k_{33}u - k_{13})z \\ (k_{24} - v) - (k_{33}v - k_{23})z \end{bmatrix} \tag{3}$$

Where (u, v) is pixel coordinate. All points on the laser steaks in the binary image can be converted to the world coordinates using equation (3), and the shape of the streak appeared on the surface object can be estimated. The global shape of an object is reconstructed by accumulating the laser streaks appeared on the surface of the object.
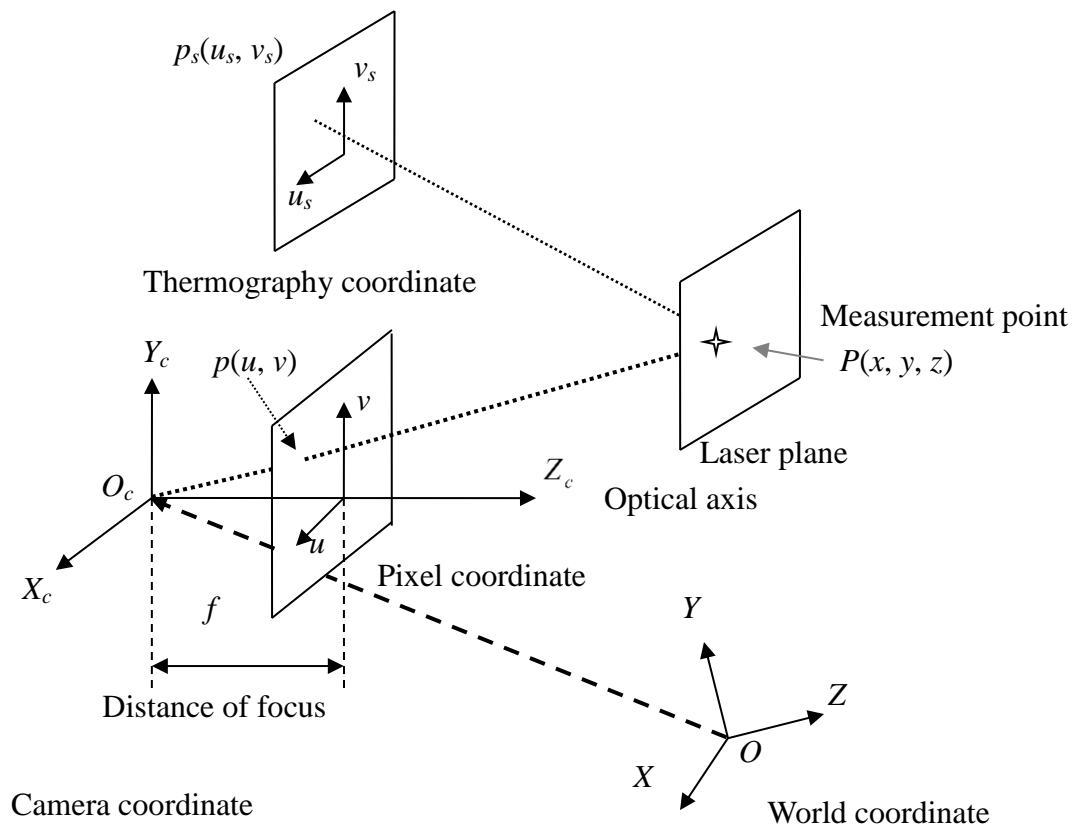
13

Fig.2-3 Relationship between pixel coordinate and world coordinate.

2.3.3 Mapping method between temperature and three-dimensional position

Since the three-dimensional shape data can be measured by the light section method, the proposed measurement system can measure not only the 3D shape of an object but also its temperature distribution by allocating the corresponding temperature data obtained by thermography to the 3D position. In addition, since the calibration block is captured by CCD camera and thermography simultaneously, the corresponding temperature data can be obtained. As shown equation (2), the relationship between the thermography coordinate (u_s, v_s) and the world coordinate (x, y, z) can be formulated as equation (4).

$$s \begin{bmatrix} u_s \\ v_s \\ 1 \end{bmatrix} = \begin{bmatrix} h_{11} & h_{12} & h_{13} & h_{14} \\ h_{21} & h_{22} & h_{23} & h_{24} \\ h_{31} & h_{32} & h_{33} & 1 \end{bmatrix} \cdot \begin{bmatrix} x \\ y \\ z \\ 1 \end{bmatrix} \tag{4}$$

Where, h_{11} to h_{33} are parameters that can be determined by inputting over 6 points into equation (4). The equation (4) can be written as follows.

$$\begin{cases} u_s = (h_{11}x + h_{12}y + h_{13}z + h_{14})/(h_{31}x + h_{32}y + h_{33}z + 1) \\ v_s = (h_{21}x + h_{22}y + h_{23}z + h_{24})/(h_{31}x + h_{32}y + h_{33}z + 1) \end{cases} \tag{5}$$

Once h_{11} to h_{33} are determined, the thermography coordinates can be calculated by inputting three-dimensional coordinates into equation (5), and the corresponding temperature data can be allocate to the reconstructed shape of a target object.

As mention in the previous section, a calibration block was used to determine camera parameters (k_{11} to k_{33}) in the system. In order to determine thermography parameters (h_{11} to h_{33}) simultaneously, the calibration block which have filaments at the each corner was made. Since the filaments generate the light and the heat, they can be as markers, and can be recorded by both the CCD camera and the thermography. The world coordinates can be easily integrated.

The flow of the measurement is shown in Fig.2-4. The laser slit ray is projected on the surface of an object and the slit laser appeared on the surface of the object is captured by CCD camera and thermography simultaneously. Then three-dimensional position of the laser streak is calculated by triangulation process. It is realized by image processing. Finally, the corresponding

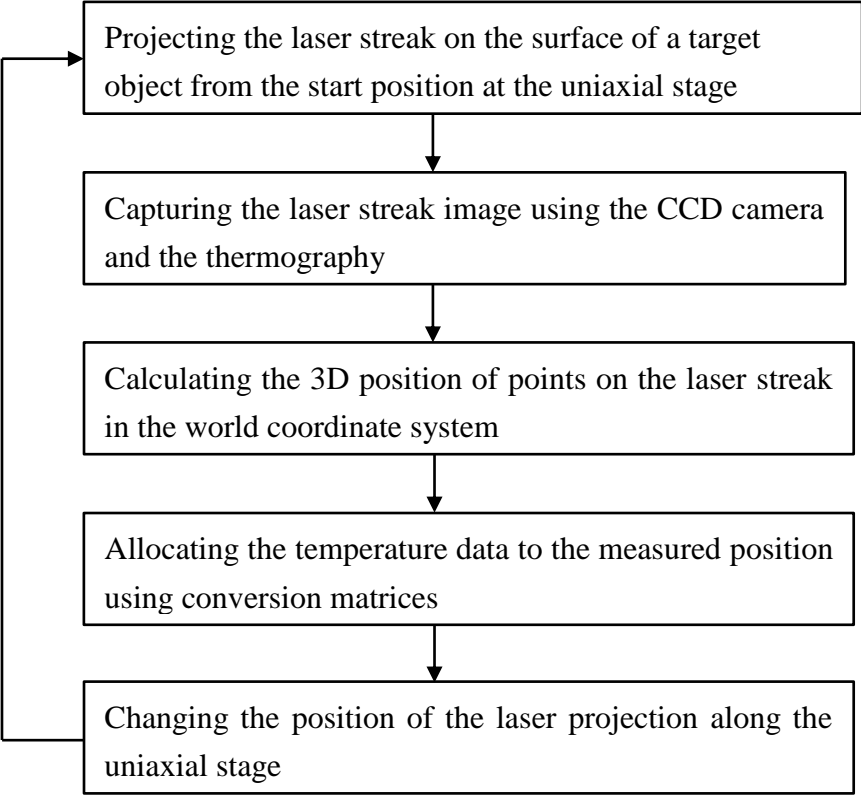temperature data obtained by thermography is allocated to the three-dimensional shape data using equation (5).

```
┌─────────────────────────────────────────────┐
│ Projecting the laser streak on the surface   │
│ of a target object from the start position   │
│ at the uniaxial stage                         │
└─────────────────────────────────────────────┘
                    │
                    ▼
┌─────────────────────────────────────────────┐
│ Capturing the laser streak image using the   │
│ CCD camera and the thermography               │
└─────────────────────────────────────────────┘
                    │
                    ▼
┌─────────────────────────────────────────────┐
│ Calculating the 3D position of points on     │
│ the laser streak in the world coordinate     │
│ system                                        │
└─────────────────────────────────────────────┘
                    │
                    ▼
┌─────────────────────────────────────────────┐
│ Allocating the temperature data to the       │
│ measured position using conversion matrices  │
└─────────────────────────────────────────────┘
                    │
                    ▼
┌─────────────────────────────────────────────┐
│ Changing the position of the laser           │
│ projection along the uniaxial stage           │
└─────────────────────────────────────────────┘
```

Fig.2-4 Flow of the measurement

2.4 Evaluation experiment

2.4.1 Accuracy evaluation

Since the size of an object projected in the image varies depending on the distance from the CCD camera to the object, and the quantitative measurement relates pixel coordinates in the image, the distance from the CCD camera to the object influences measurement accuracy. Therefore, measurement accuracy for distance is carried out. In order to evaluate the measurement accuracy, a cube block is used in this study, and is shown in Fig.2-5. Size of the block is 147.8mm x 97.9mm x 62.4mm. Precision evaluation was executed by taking a difference between the measured value and the intrinsic dimensions at various distances from 400mm to 1200mm at 100mm intervals. The 3D shape of the block is shown in Fig.2-6 (away 800 mm). Measurement accuracy is shown in Fig.2-7. When the distance from the CCD camera to the object was not 800mm, the error was less than 1mm.

Fig.2-5 Measurement object

* Point 1 : 43.88065, 47.89738, 171.00101
* Point 2 : 140.63783, 48.91013, 168.00090
* Distance : 96.80898 mm
* Displacement : 96.75718, 1.01275, -3.00011
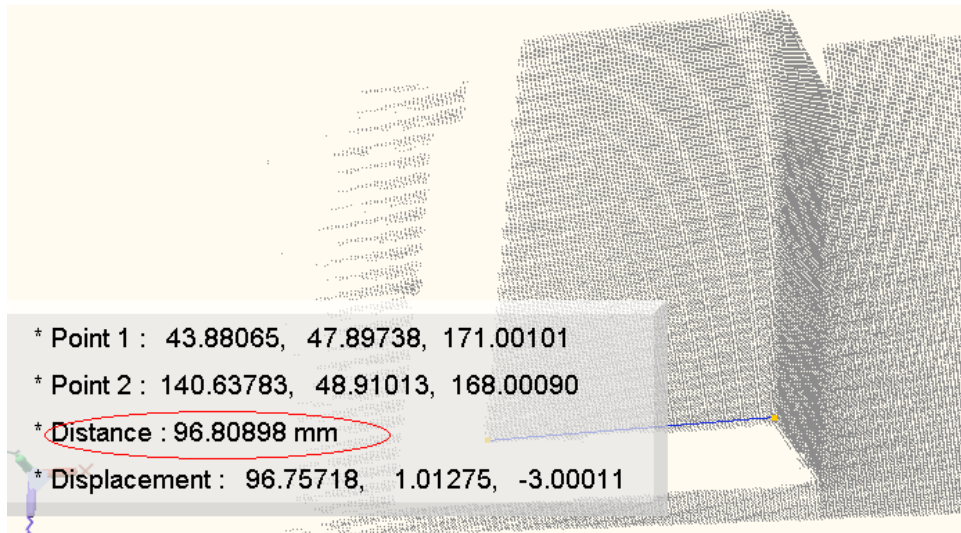
Fig.2-6 Reconstructed 3D shape of the block
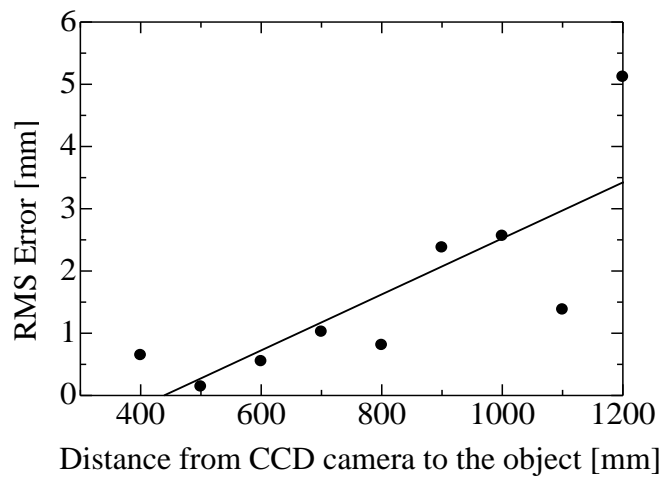
Fig.2-7 Measurement accuracy

2.4.2 Measurement result

In this study, measurement result of a human hand was introduced for one of the examples of the 3D temperature measurement. Fig.2-8 shows the 2D thermal image. The red points appeared in thermal image are filaments. The red points were used to match the coordinates between the pixel coordinate and the world coordinate (or between the thermography coordinate and the world coordinate). Fig.2-9 shows the measurement result.
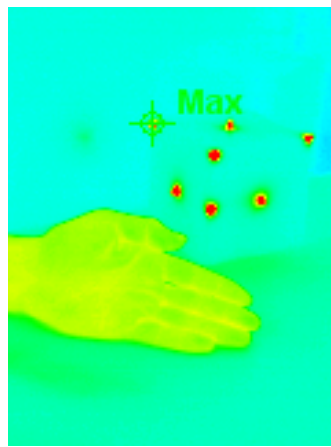
Fig.2-8 thermal image
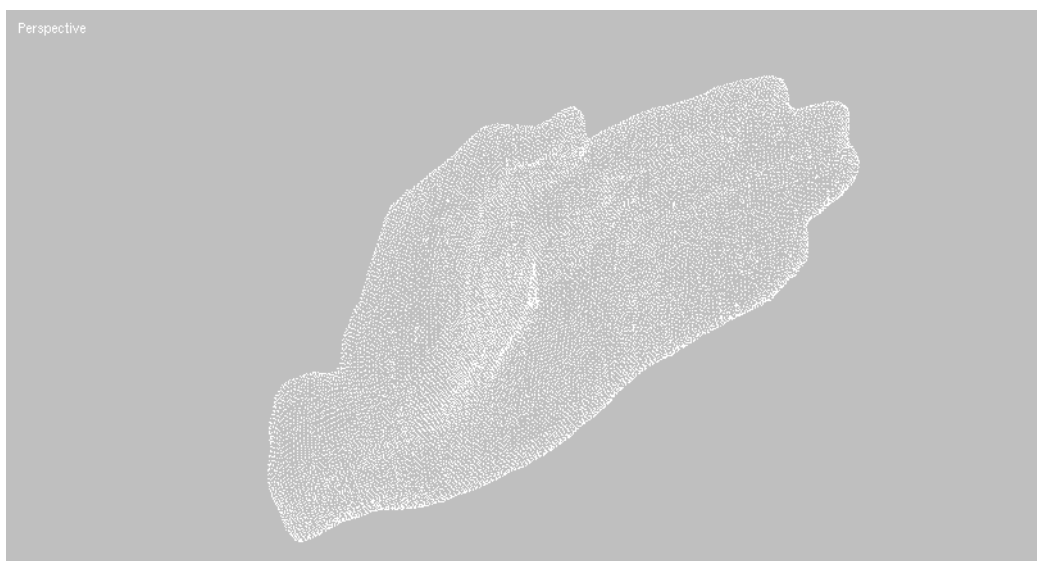
Fig.2-9a Point cloud data

Fig.2-9b Polygon data
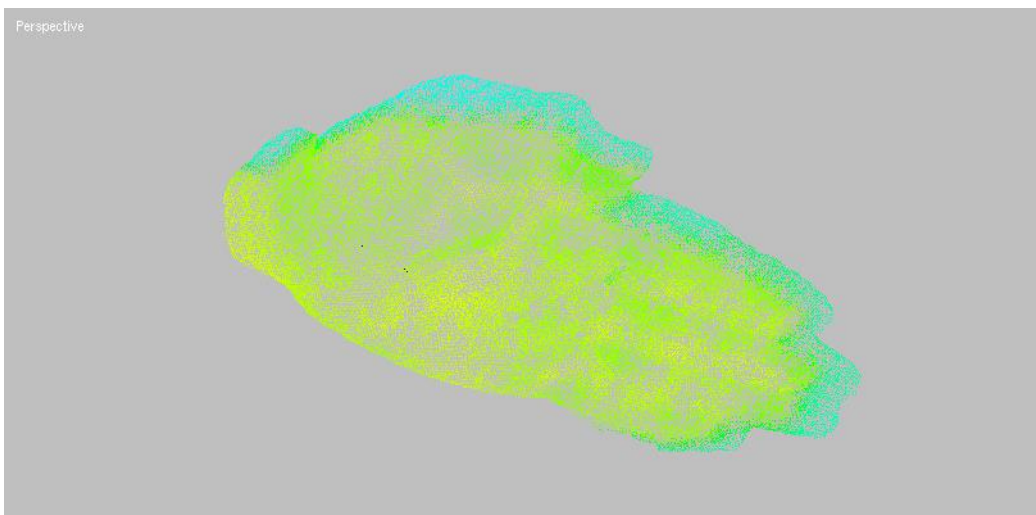
Fig.2-9c Measurement result of a human hand

Although original 2D image has not quantitative information such as the size and the position of heat source, quantitative analysis can be carried out by acquiring three-dimensional temperature distribution data of a target object.

2.5 Conclusion

In this study, the subjacent measurement method that can obtain 3D temperature distribution of an object was introduced. The proposed measure system was established by combining a thermography with a three-dimensional shape measurement method by laser (light section method). Here, the light-section method was realized by moving the slit laser projector equipped on a uniaxial stage. In order to acquire 3D temperature distribution, a calibration method was introduced. In addition, in order to allocate the corresponding temperature data to the three-dimensional position, a mapping method was proposed.

Generally, two-dimensional images recorded from different angles cannot be connected each other, but the three-dimensional data can be connected by adjusting the coordinates on a computer. Therefore, a high resolution model can be reconstructed by connecting the three-dimensional shape data obtained from different angles.

CHAPTER 3: System development using a handheld 3D measuring instrument

3.1 Introduction

All objects emit electromagnetic radiation. The relationship between the absolute temperature of an object and the intensity and wavelength of the emitted radiation is defined by the Stefan-Boltzmann Law. Over the past 50 years, numerous studies, particularly the correlation between temperature patterns and medical conditions in humans and animals, have been conducted [20]-[21]. In medicine, thermography is an important measurement tool for evaluating the state of human health through careful analysis of skin surface temperatures [22]-[23]. However, since thermal images captured by thermography are two dimensional, 3D temperature distribution cannot be confirmed. In addition, the device proposed in Capture 2 cannot measure the back of the target object using the light-section method because the back of the object cannot be observed by the camera.

Therefore, in order to address these problems, a measurement system composed of a portable 3D instrument (Kinect sensor) and an infrared thermography device is proposed. Measurement of 3D thermogram is realized by mapping thermal data obtained by thermography to 3D position information obtained by a portable Kinect sensor. Integrating 3D scanning techniques with thermograms can help to create standardized thermograms [24]. Although reference paper in relation to 3D temperature distribution is very poor, a large number of portable 3D scanning techniques have been reported [4]-[5][25] -[28]. The author [26] presents a 3D measuring device (Kinect sensor) that can detect the motion and posture of a human body without the need for any special tools or equipment because it contains a distance sensor and an image sensor. The processor at the heart of the Kinect sensor enables the positions of the joints of the body to be estimated using information input from the sensor. Moreover, the Kinect sensor can measure the 3D surface shape of an object instantaneously. Using the 3D shape data acquired by the Kinect sensor, it is possible to obtain quantitative information that includes shape and temperature

distribution information by combing thermography. Three-dimensional thermograms can be easily obtained and can be performed automatically using the proposed mapping method. This Chapter proposes a measurement model that combines 3D scanning methods and thermal imaging to produce standardized 3D thermograms and integrates new approaches to temperature distribution data analysis and visual analytics based on 3D thermograms. Based on the proposed mathematical model, it is possible to detect not only the 3D shape of an object, but also its temperature distribution. When the instrument is moved, the entire perimeter of the target object can be automatically measured by splicing the obtained shape data using the iterative closest point (ICP) algorithm. The entire 3D shape of the object can be reconstructed using this algorithm. Such a system provides a new basis for medical applications based on non-invasive diagnostic methods.

3.2 Configuration of measurement system

The proposed measurement system is established using a portable 3D instrument (Kinect sensor) and an infrared thermography which are unified. The measurement system is shown in Fig.3-1. The portable 3D instrument consists of an infrared laser projector, an infrared camera and an RGB camera. Depth information can be obtained by triangulation process. Specifically, in order to obtain the depth information, a constant pattern of speckles created by the laser source is projected onto the scene and recorded by the infrared camera. Then, this pattern is correlated against a reference pattern. The reference pattern is obtained by capturing a plane at a known distance from the sensor. As a speckle is projected on an object, the position of the speckle in the infrared image is shifted in the direction of the baseline between the laser projector and the perspective center of the infrared camera. All shifts of speckles are measured by the image correlation procedure, which yields a disparity image. Each pixel at a distance to the sensor can be corrected from the corresponding disparity. Fig.3-2 illustrates the depth measurement from the infrared image and the depth image [27]-[29].

On the other hand, infrared thermography can capture two-dimensional thermal image. The Size of the thermal image is 320 x 240 pixels. In order to capture one frame, it takes 1/60 second. Fig.3-3 shows an example of thermal images captured by the thermography.
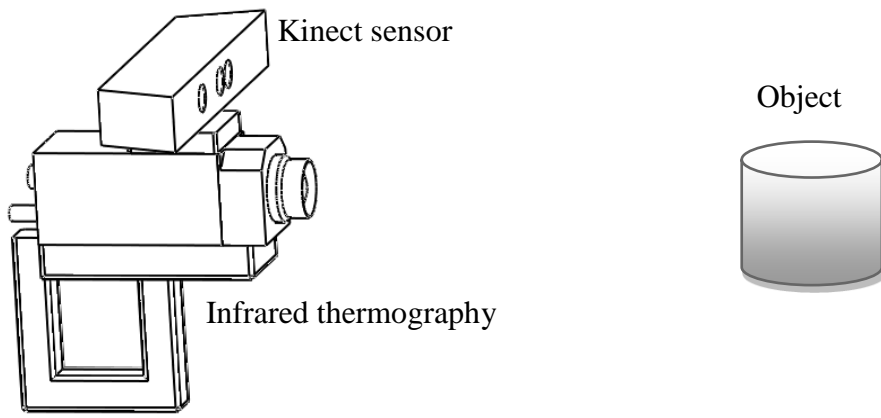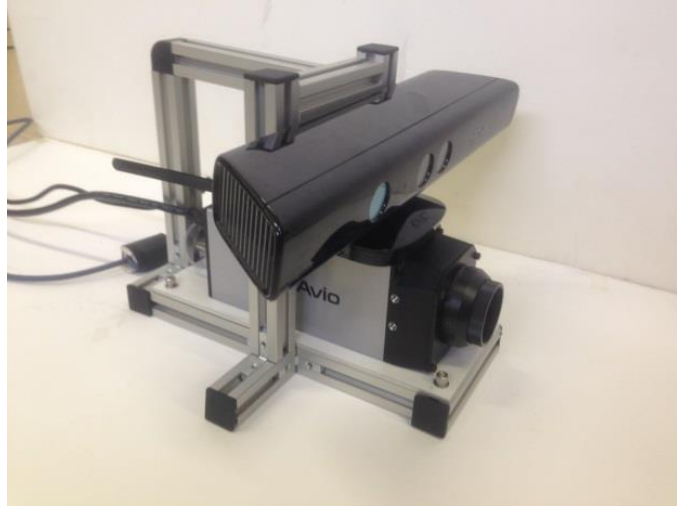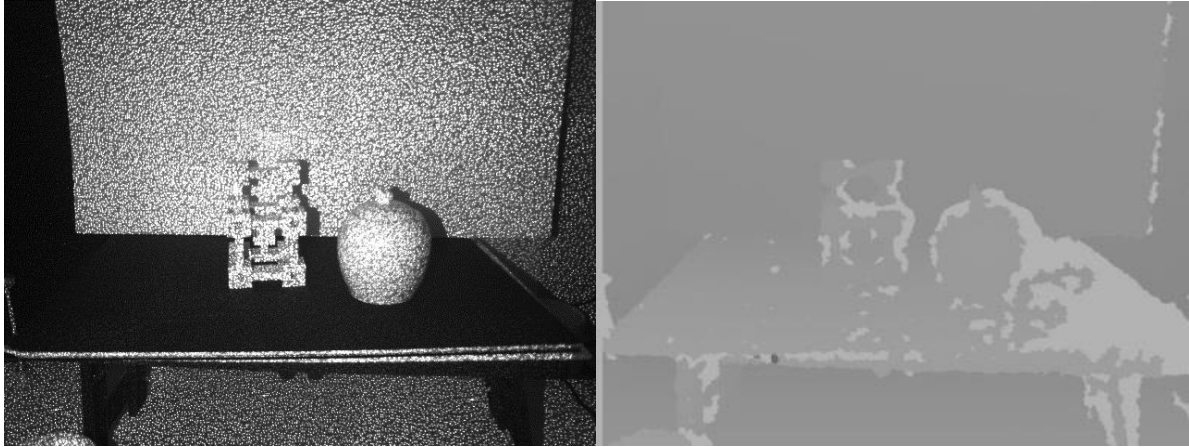
Kinect sensor

Object

Infrared thermography

Fig.3-1 Measurement system.

(a) Infrared image   (b) Depth image

Fig.3-2 Depth measurement from the infrared image and the depth image
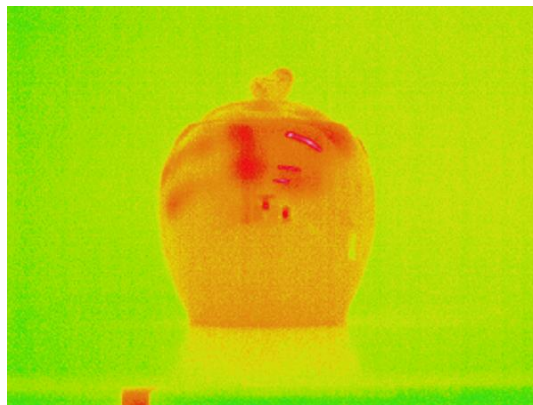

Fig.3-3 An example of thermal image.

As shown in Fig.3-2, images recorded by the infrared camera are depth images that show the depth information of measurement points with a brightness level. The size of the depth image is 640 x 480 pixels, and the harmony per one pixel is 16 bits. Three-dimensional coordinates of measurement points projected on the surface of an object are calculated by triangulation process. 3D coordinates of the measurement points are expressed as a world coordinate system with its origin at the perspective center of the infrared camera on the Kinect sensor. As shown in Fig.3-4, the Z axis is orthogonal to the image plane towards the object, and the X axis is perpendicular to the Z axis in the direction of the baseline between the infrared camera center and the laser projector, the Y axis is orthogonal to X and Z, making a right-handed coordinate system. Fig.3-5 shows the three-dimensional shape of an object measured by the Kinect sensor. The pixel coordinates in the depth image can be converted to the three-dimensional coordinates using equation (6).

$$\begin{cases} x = \frac{d[u,v]}{F} \cdot ps \cdot (u - 320) \cdot 2 \cdot 0.001 \ [m] \\ y = \frac{d[u,v]}{F} \cdot ps \cdot (v - 240) \cdot 2 \cdot 0.001 \ [m] \\ \qquad z = d[u,v] \cdot 0.001 \ [m] \end{cases} \tag{6}$$

Where (u, v) are the pixel coordinates in the depth image, and $d[u, v]$ is the value of the brightness level in the depth image, and F is the focus of the infrared camera, and ps is a constant parameter.

Fig.3-6 shows the flow of the measurement. When a target object is measured by using this system, calibration of the thermography should be carried out in advance. The 3D shape of the target object can be measured by the Kinect sensor, and the thermal image of the object is recorded by thermography simultaneously. Then, the corresponding temperature data is allocated to the 3D surface shape of the measurement object using calibration parameters (as mentioned in the next section).
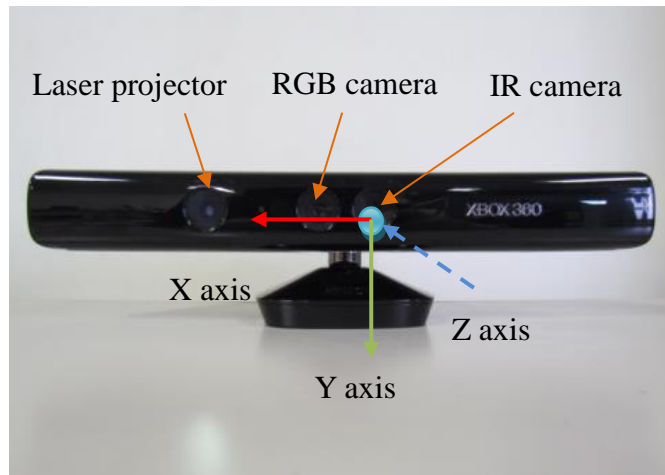
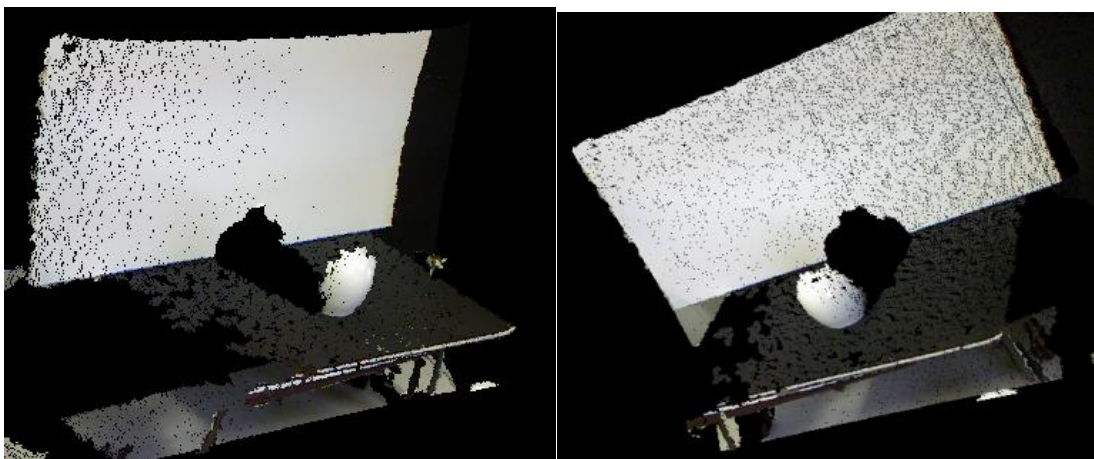**Fig.3-4**Originof the world coordinates on the Kinect sensor
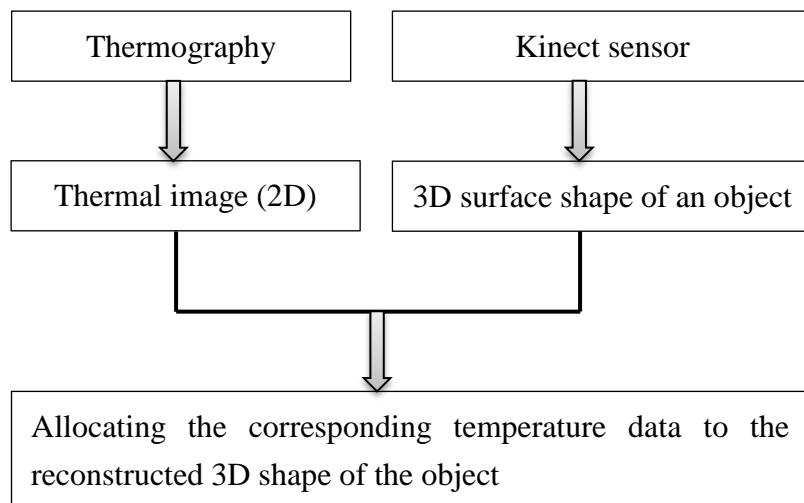

Fig.3-5 3D shape of an object.

```
┌─────────────────────┐        ┌─────────────────────┐
│    Thermography     │        │    Kinect sensor    │
└─────────────────────┘        └─────────────────────┘
           ⇓                              ⇓
┌─────────────────────┐        ┌─────────────────────────────┐
│ Thermal image (2D)  │        │ 3D surface shape of an object│
└─────────────────────┘        └─────────────────────────────┘
                      ⇓
┌─────────────────────────────────────────────────────────┐
│ Allocating the corresponding temperature data to the     │
│ reconstructed 3D shape of the object                      │
└─────────────────────────────────────────────────────────┘
```

Fig.3-6 Measurement flow

3.3 Measurement principle

3.3.1 Method of image processing

In this study, shading processing and smoothing processing of image are carried out. The shading processing is a method that can give a three-dimensional impression with shading information to the surface of the object. A small plane is made by using the three adjacent pixels and the brightness information of the pixel from angle between normal vector of the plane and the light source vector. Fig.3-7 shows the mechanism of shading and Fig.3-8 shows the shading image. The smoothing processing of image is a technique that is used to smooth flat luminance values of the image. The value of the target pixel is replaced by the average value of the distance data using 9 pixels in total. Fig.3-9 shows the smoothing result of image.
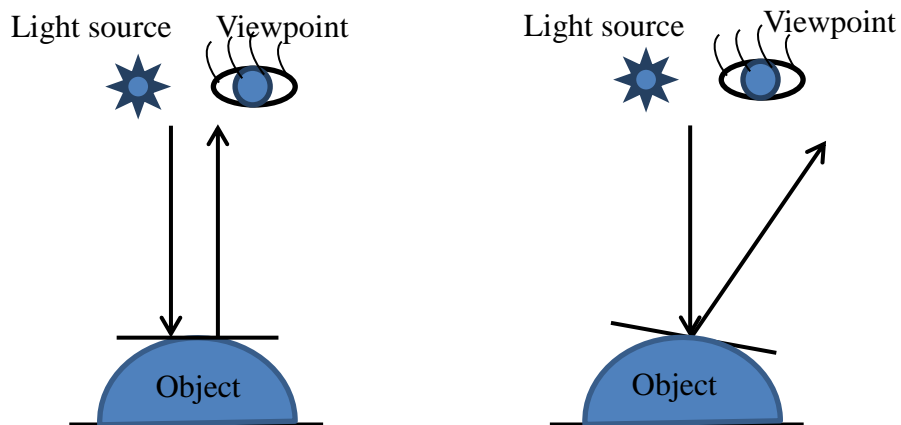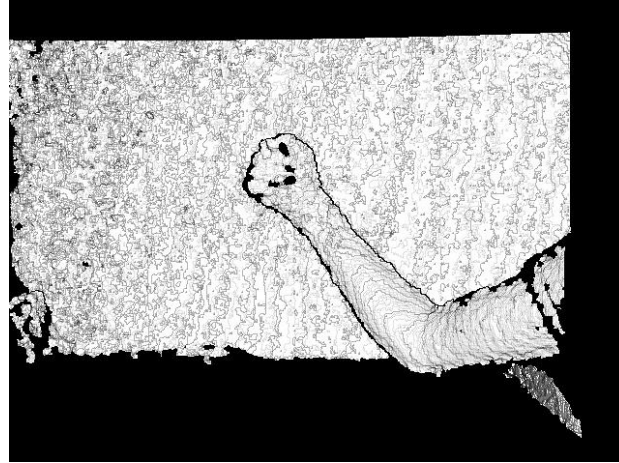

Fig.3-7 Mechanism of shading
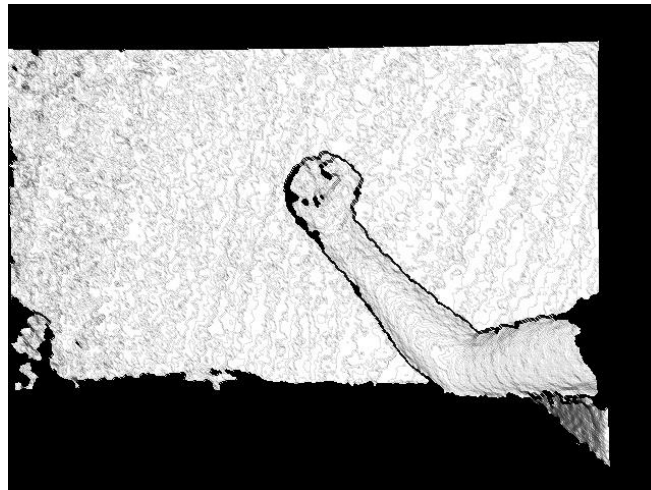
Fig.3-8 Shading image

Fig.3-9 smoothing result of image

3.3.2 Calibration method

In order to measure the 3D surface temperature of a target object, calibration of the thermography has to be carried out in advance. A calibration block is used to match the coordinates between the world coordinate system and the thermography coordinate system since thermal-image can be recorded by thermography. The calibration setup is shown in Fig.3-10. The 3D surface shape of the block is measured by the Kinect sensor, and the thermal- image of the block is recorded simultaneously by thermography since the recorded thermal-image is used to determine the calibration parameters.

The relationship between the thermography coordinates (u_s, v_s) and the world coordinates (x, y, z) can be formulated as follows.

$$s \begin{bmatrix} u_s \\ v_s \\ 1 \end{bmatrix} = \begin{bmatrix} h_{11} & h_{12} & h_{13} & h_{14} \\ h_{21} & h_{22} & h_{23} & h_{24} \\ h_{31} & h_{32} & h_{33} & 1 \end{bmatrix} \cdot \begin{bmatrix} x \\ y \\ z \\ 1 \end{bmatrix} \tag{7}$$

Where h_{11} to h_{33} are calibration parameters that consider the rotation, scale and displacement between the thermography coordinate and the world coordinate. These parameters (h_{11} to h_{33}) can be determined by inputting by inputting no less than 6 corresponding points into equation (7). Equation (7) can be written as follow.

$$\begin{cases} u_s = (h_{11}x + h_{12}y + h_{13}z + h_{14})/(h_{31}x + h_{32}y + h_{33}z + 1) \\ v_s = (h_{21}x + h_{22}y + h_{23}z + h_{24})/(h_{31}x + h_{32}y + h_{33}z + 1) \end{cases} \tag{8}$$

Once h_{11} to h_{33} are determined, the thermography coordinates can be calculated by inputting 3D coordinates of the points projected on the surface of an object into equation (8). Then the corresponding temperatures can be allocated to the reconstructed surfaces of the object.
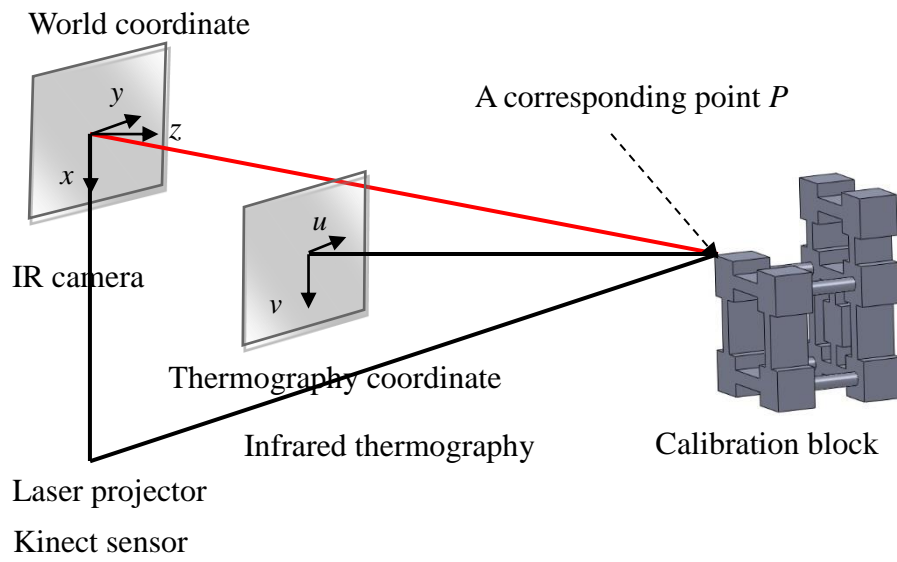
World coordinate

A corresponding point P

y

z

x

IR camera

u

v

Thermography coordinate

Infrared thermography

Laser projector

Kinect sensor

Calibration block

Fig.3-10 Calibration setup

3.3.3 ICP (Iterative Closest Point) algorithm

In order to measure the global 3D surface temperature of an object, ICP algorithm is used in our system. When the instrument is moved, the entire perimeter of the target object can be automatically measured by splicing the obtained shape data using this algorithm. Many studies about ICP technique have been reported [30]-[31]. However, these methods have some problems that it takes a long time to perform and error often occurs in the matching result. For example, the author [31] presents a colour ICP method using texture information. An accurate scan matching is realized by combining shape and colour information with feature value than normal ICP method. But mapping accuracy is affected by light.

This Chapter proposes a new ICP method by a multisport laser. The multisport laser is projected on the surface of a target object, and Kinect sensor measures the 3D shape of the target object at different positions. In order to connect two point cloud data acquired by the Kinect sensor, it is necessary to extract the 3D coordinates of the laser points on the surface of the target object. Connection of point data can be realized by calculating the movement and the rotation angle of the laser points. Fig.3-11 shows two point cloud data obtained at different positions. Fig.3-12 shows connection of two point cloud data. Three-dimensional thermal image is shown in Fig.3-13. The common area has to be included in each data. These point cloud data can be connected using ICP algorithm as shown in Fig.3-14.
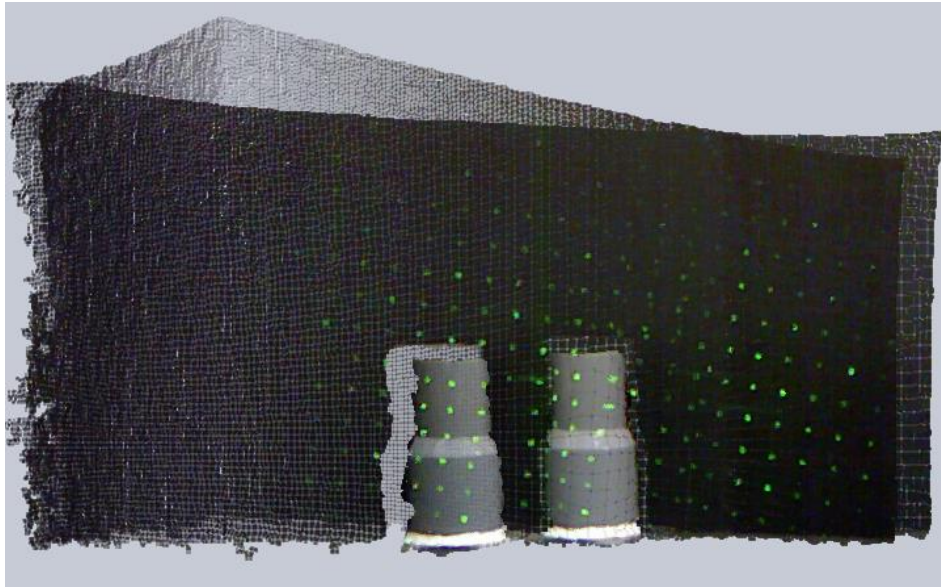
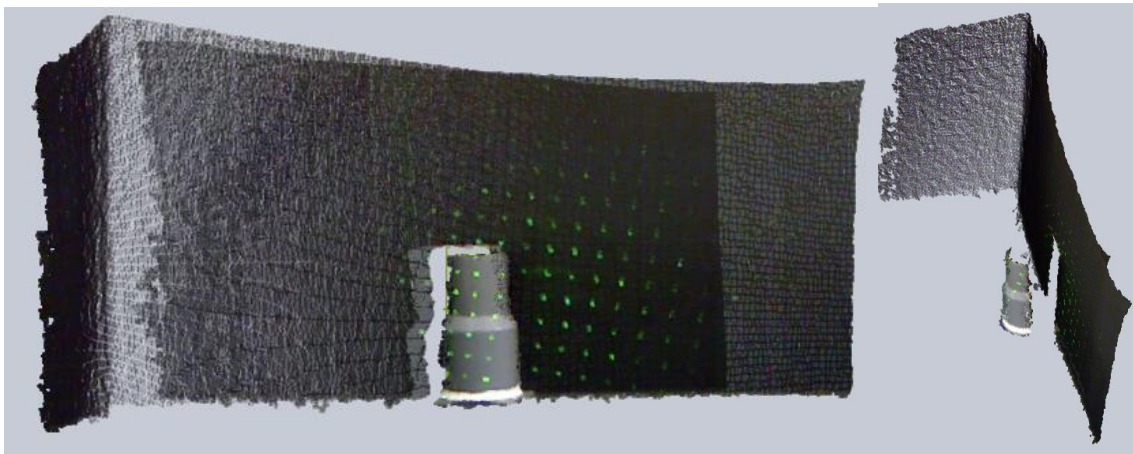**Fig.3-11** Point cloud data obtained at different positions

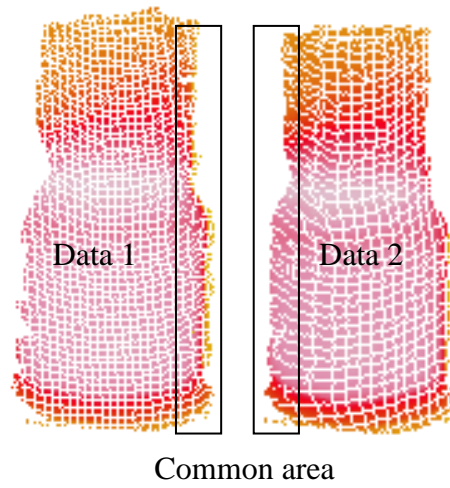**Fig.3-12** Connection of two point cloud data

Fig.3-13 Three-dimensional thermal image obtained at different positions

Fig.3-14 Connection of two 3D data

3.4 Evaluation experiment

3.4.1 Accuracy evaluation

Since the size of the object appearing in the IR camera image varies depending on distance from the Kinect sensor to the object, and quantitative measurement is obtained from the depth image, the distance from the Kinect sensor to the target object influences measurement accuracy and connection accuracy. Because even if ICP algorithm is used, two point cloud data cannot be connected correctly if one point cloud data was obtained near the target object and the other was obtained farther away the target object.

Therefore, measurement accuracy is evaluated by changing the distance from the Kinect sensor to the target object. To verify the relation between random error and the distance from the Kinect sensor, a flat board with scale was measured and the precision evaluation was carried out at various distances from 50cm to 400cm at 50cm intervals. The measurement accuracy is shown in Fig.3-15.When the distance of the object from the Kinect sensor was not over 100cm, the error was less than 5mm.
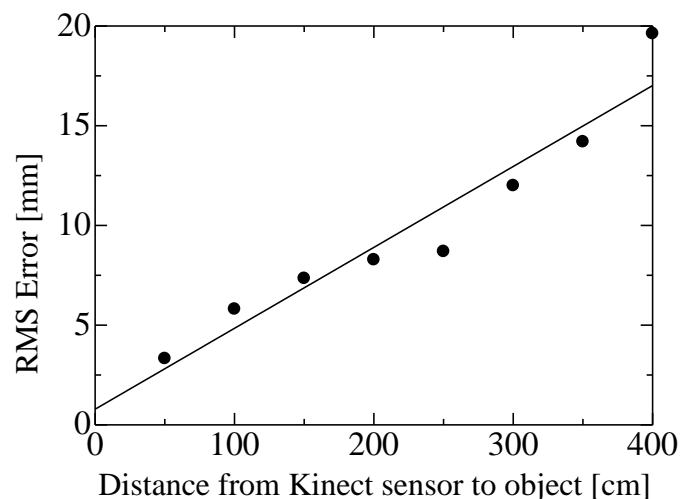

Fig.3-15 Measurement accuracy

3.4.2 Measurement result

In order to show the effectiveness of the proposed measurement device, a cylinder part was measured. Measurement result of a resin part is introduced for one of the examples of the 3D temperature measurement. The photograph of the resin part and the 2D thermal-image are shown in Fig.3-16.The reconstructed 3D temperature distribution is shown in Fig.3-17. It was confirmed by the experimental result that the proposed system can measure the global 3D temperature distribution of a target object using the iterative closest point (ICP) algorithm. Although the original 2D image does not have quantitative information such as the size and the position, 3D thermal data obtained by the proposed system can be connected using ICP algorithm.
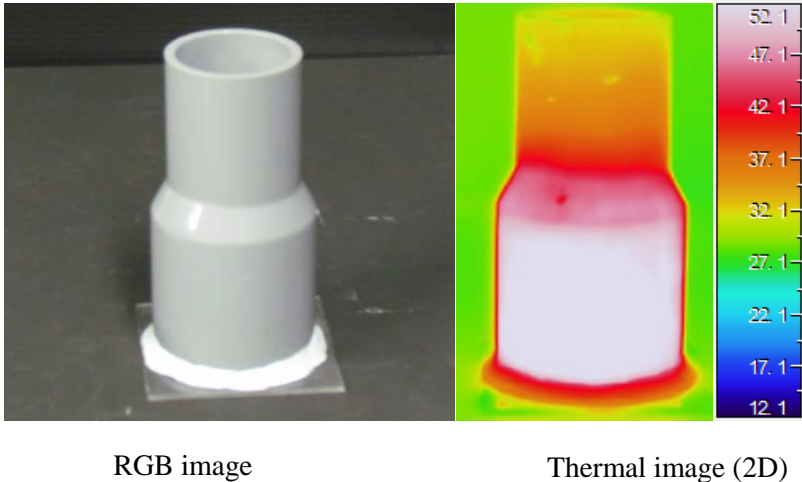

RGB image   Thermal image (2D)

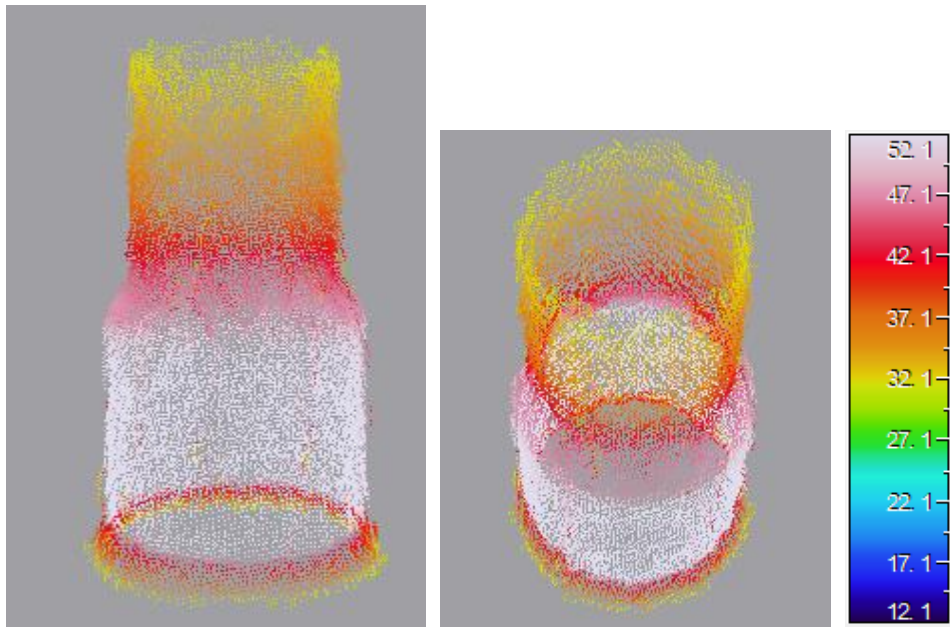**Fig.3-16** Images by CCD camera and thermography

Fig.3-17 Reconstructed 3D temperature distribution

3.5 Conclusion

In this Chapter, a measurement system that was composed of a handy type three-dimensional measuring instrument (Kinect sensor) and an infrared thermography was proposed. Measurement of 3D temperature distribution was realized by mapping thermal data obtained by thermography in three-dimensional position obtained by the handy type three-dimensional measuring instrument. Generally, 2D thermal images recorded from different angles cannot be connected by each other, but the 3D shape data can be connected by adjusting the 3D coordinates on a computer. The feasibility of the proposed system was confirmed by experiment. Since the system can detect the three-dimensional shape and the temperature distribution of an object simultaneously, it can be a valuable model for current and future applications for modelling and simulating biological and physiological processes of the human body.

This concept is defined by the 3D thermo-sensing system presented three processes, calibration method, mapping method and medical applications. These processes provide novel framework for development of 3D physiological models and techniques for their analysis and visualization.

In this study, since the 3D thermal data can be connected by each other, a high-resolution model can be reconstructed using the 3D data obtained from different angles. It will be future work to enhance acquisition of 3D thermograms in real-time. Thus different ways of data analysis and data visualization will be explored for developing 3D thermogram analysis, visual analysis and visualization tools used in different applications.

CHAPTER 4: Research on high accuracy by combining a light-section method and a magnetic sensor

4.1 Introduction

This Chapter presents an investigation of the geometric quality of 3D data obtained using a 3D thermal-sensing system. Since this system is composed of a 3D measurement device and a thermographic device, the system can detect not only the 3D shape of an object but also its temperature distribution. In general, the 3D shape of an object is measured by either a light-section method or a stereo vision method [32]-[36]. Quantitative measurement is established by considering the geometric configuration between a CCD camera and a structured light or two CCD cameras. A handheld measurement system using the stereo vision method was proposed in a previous study [36]. However, occlusion problem can easily occur when using the stereo vision method. Areas that cannot be measured exist in numerous cases if the object includes complex regions.

The circumferential shape of the entire object can be measured using the method proposed in Chapter 3. However, the measurement accuracy depends on the performance of the 3D measuring instrument. In order to improve the measurement accuracy and cope with the problem as shown above, a system that can maintain the proper angle between the laser-projection unit and the image-capture unit (i.e., the CCD camera and the thermography device) was proposed. The laser-projection unit and the image-capture unit can be moved freely by mounting magnetic sensors on them, thus allowing real-time operation by maintaining the proper angle against form of the target object. This enables portable scanning measurements to be performed. Therefore, the proposed system can measure 3D temperature distribution of an object regardless of the shape and the size of an object. In addition, the occlusion problem can be solved by scanning the surface of an object freely. Here, the magnetic sensors detect the 3D position and orientation of the image-capture unit and the slit laser projector at a rate of 60 Hz.

In order to measure the 3D temperature distribution of an object, it is necessary to record a thermal image of the object when the laser streak points projected on the surface of the object are extracted. Thus, the corresponding temperature data can be allocated to the 3D surface shape of the object. An allocation method to convert from moving coordinates to thermography coordinates was proposed. The relationship between the moving coordinate system and the thermography coordinate system is formulated using conversion matrix. Once the 3D coordinates of the object points are measured, the corresponding temperatures can be allocated to the 3D surface shape of the object using the matrix.

4.2 Configuration of measurement system

Fig.4-1 shows the measuring system. The measuring system is established using a 3D measurement device and a thermography. The 3D measurement device consists of a CCD camera, a slit laser which magnetic sensors were mounted on them. The CCD camera and the thermography, called image detecting unit, are unified and separated from the laser projector. The magnetic receivers were mounted on each of the image detecting unit and the slit laser projector to realize handy scanning measurement. The transmitter of the magnetic sensor generates the magnetic field, and the signal detected by the magnetic receiver is sent to the main controller to calculate the three-dimensional information of the magnetic receiver. This information contains three-dimensional position parameter and rotational motion parameter. Here, the positions and the orientations of the image detecting unit and the slit laser projector are detected at a rate of 60 Hz during the measurement. In order to measure three-dimensional temperature distribution of an object, the slit ray is projected on the surface of the object, and the laser streak is observed and recorded by a CCD camera and a thermography simultaneously. Then the 3D shape of the target object is calculated by triangulation process and the corresponding temperature is allocated to the 3D shape using conversion matrix. Here, it is necessary to determine the conversion matrix in advance. Elements of the conversion matrix are determined by calibration process.
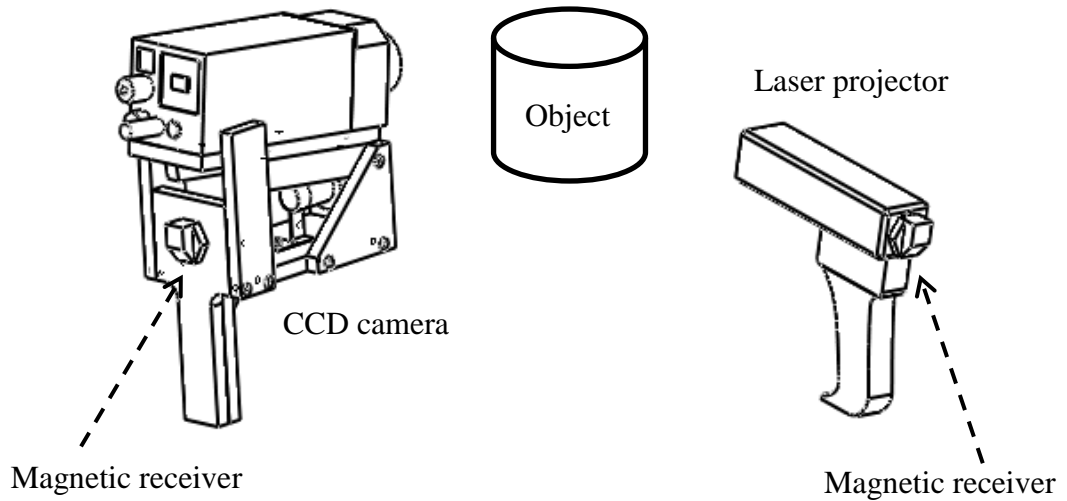
Thermography

Object

Laser projector

CCD camera

Magnetic receiver

Magnetic receiver
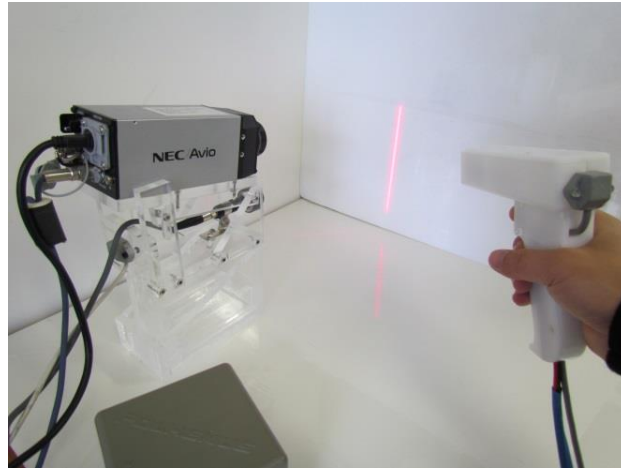
Fig.4-1 Measurement system

4.3 Proposal of three-dimensional measurement method

Fig.4-2 shows relationship between the moving coordinate system and the fixed coordinate system. As shown in Fig.4-2, a measurement point (P) is located as the intersection between the laser plane and the vector from focal point. The 3D coordinate of the measurement point (P) is expressed as a moving coordinate system with its origin at the electrical center of the receiver of magnetic sensor. Its 3D coordinate is expressed as $M_r=[x_r, y_r, z_r]^t$. On the other hand, electrical center of the transmitter is expressed as origin of a fixed coordinate system. So, the fixed coordinate of the measurement point (P) is expressed as $M_w=[x, y, z]^t$. The positional relationship between the fixed coordinate system and the moving coordinate system is formulated as equation (9).

$$M_w = R \cdot M_r + t \tag{9}$$

Where R is a rotation matrix and t is a translation vector. Therefore, the 3D shape of the target object can be integrated in the fixed coordinate system by coordinate transformation and detecting the rotation matrix R and the translation vector t on every measurement. The rotation matrix R and the translation vector t are detected in real-time by magnetic sensors.

In order to realize this arithmetic processing, it is performed as follow: First of all, three-dimensional measurement is carried out by using light-section method. Here, the position posture of image detecting unit and the laser projector is detected in real-time by the magnetic sensors. Then the 3D coordinates of the object points is integrated from the moving coordinate system into the fixed coordinate system on every measurement. Finally, the corresponding temperature is allocated to the three-dimensional shape of the measurement object using conversion matrix.

In this system, the 3D coordinates of the laser streak points are measured by triangulation process. The relationship between the pixel coordinate $[u, v]$ in RGB image and the moving coordinate $[x_r, y_r, z_r]$, and the laser plane expressed in the moving coordinate system can be formulated as equation (10).

$$\begin{cases} s \cdot \tilde{m} = A[x_r \quad y_r \quad z_r \quad 1]^T \\ a \cdot x_r + b \cdot y_r + c \cdot z_r = 1 \end{cases} \qquad (10)$$

Where s is scale factor of RGB image, and $\tilde{m}$ is homogeneous coordinates $[u, v, 1]^t$ of pixel coordinates (u, v), and A is 3x4 conversion matrix which contains characteristic of CCD camera, rotation matrix and translation vector, and a, b, c are constant parameters that can be determined by inputting 3 points into the laser plane equation.
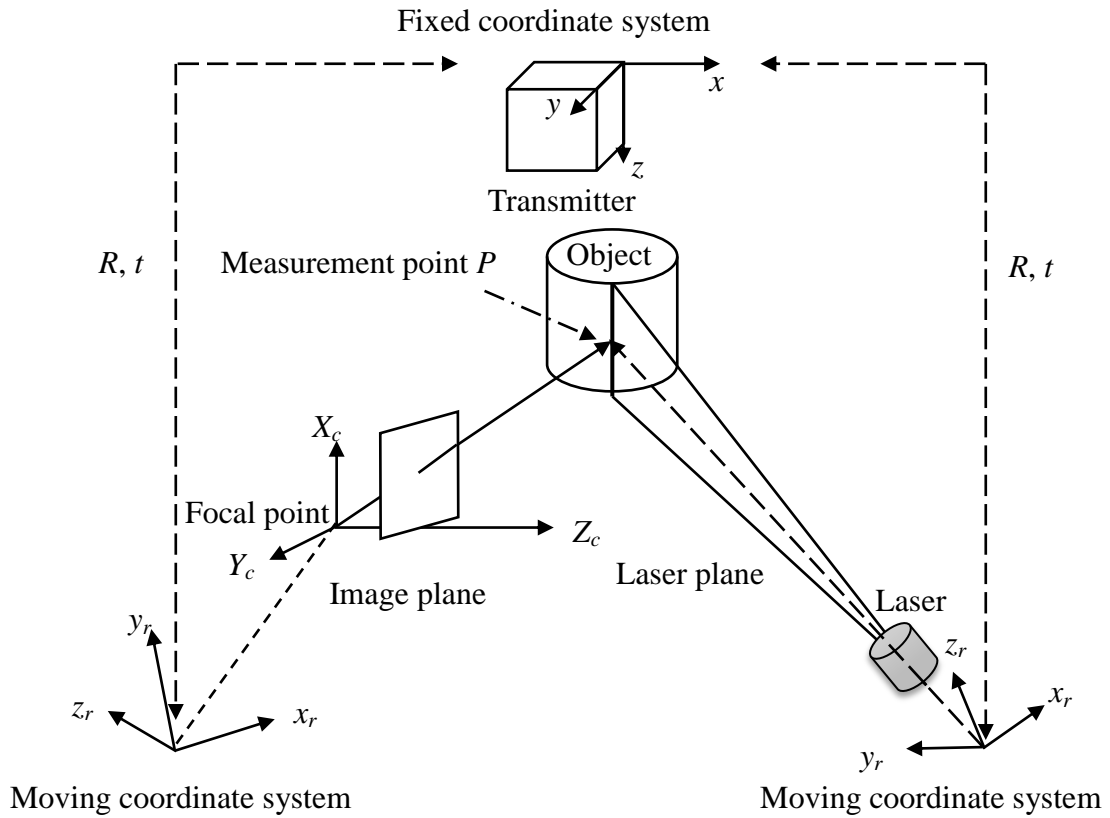

Fig.4-2 Relationship between the moving coordinate system and the fixed coordinate

4.4 Measurement principle

4.4.1 Calculation of laser plane

Fig.4-3 shows the relationship between the laser plane and the fixed coordinate system. In order to realize the 3D measurement while moving the laser projector, it is necessary to determine the equation of the laser plane in advance. Although the laser plane expressed at the moving coordinate system can be determined easily, it is necessary to determine the laser plane expressed at the fixed coordinate system since the global 3D temperature distribution of a target object at the fixed coordinate system is measured finally. Equation of the laser plane is expressed as follows.

$$A \cdot x + B \cdot y + C \cdot z = 1 \tag{11}$$

As shown in Fig.4-3, laser plane is parallel to the plane (z_r, x_r). A, B, C are constant parameters that can be determined by inputting 3 points at the moving coordinate system. In order to determine the laser plane, it is necessary to convert the moving coordinates of the 3 points into the fixed coordinates. As shown equation (9), the positional relationship between the fixed coordinate system and the moving coordinate system is formulated as equation (12).

$$M_w = R \cdot M_r + t \tag{12}$$

Where, $M_r = [x_r, \ y_r, \ z_r]^t$ means the moving coordinate, and $M_w = [x, \ y, \ z]^t$ means the fixed coordinate. Once the moving coordinates of 3 points are converted into the fixed coordinates by equation (12), parameters (A, B, C) can be determined by equation (11). Here, the position relationship between the parameters (A, B, C) and the fixed coordinates is expressed as follows.

$$\begin{bmatrix} x_1 & y_1 & z_1 \\ x_2 & y_2 & z_2 \\ x_3 & y_3 & z_3 \end{bmatrix} \cdot \begin{bmatrix} A \\ B \\ C \end{bmatrix} = \begin{bmatrix} 1 \\ 1 \\ 1 \end{bmatrix} \tag{13}$$
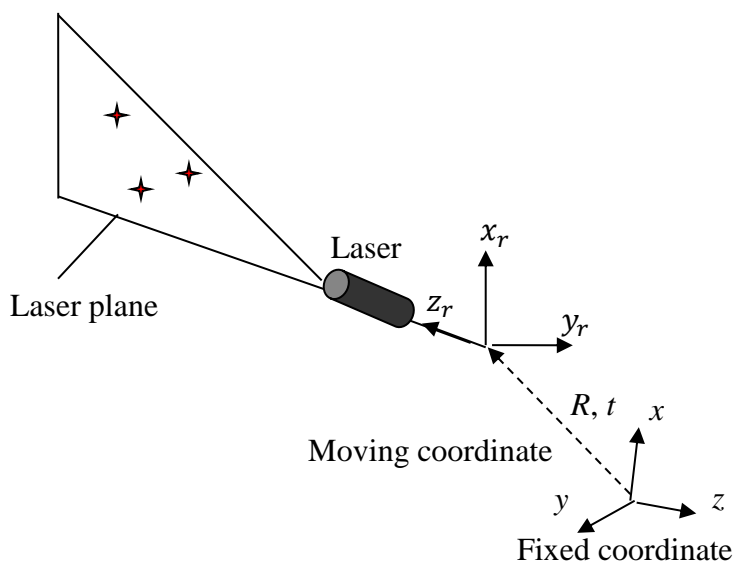
Fig.4-3 Relationship between the laser plane and the fixed coordinate system.

4.4.2 Calibration method

In order to measure the 3D temperature distribution of an object, calibration of CCD camera and thermography must be carried out in advance as mentioned before. Fig.4-4 shows calibration setup. In this study, a calibration board is used to match the coordinates between the moving coordinate system and the pixel coordinate system (or between the moving coordinate system and the thermography coordinate system). Some smaller holes are drilled in the calibration board at the position becoming the standard. Because it is necessary to capture images (thermal-image and RGB image) for calibration, and integrate into the moving coordinate system. Fig.4-5 shows calibration images. As shown equation (2), the relationship between the thermography coordinates $[u_t, v_t]$ and the moving coordinate $[x_r, y_r, z_r]$ (or the relationship between the pixel coordinate $[u, v]$ and the moving coordinate $[x_r, y_r, z_r]$) can be formulated as equation (14). Fig.4-6 shows the relationship between these coordinate systems.

$$s \begin{bmatrix} u_t \\ v_t \\ 1 \end{bmatrix} = \begin{bmatrix} h_{11} & h_{12} & h_{13} & h_{14} \\ h_{21} & h_{22} & h_{23} & h_{24} \\ h_{31} & h_{32} & h_{33} & 1 \end{bmatrix} \cdot \begin{bmatrix} x_r \\ y_r \\ z_r \\ 1 \end{bmatrix} \tag{14}$$

Where h_{11} to h_{33} are calibration parameters that consider the rotation, scale and displacement between the thermography coordinates (the pixel coordinates) and the moving coordinates. These parameters are the elements of conversion matrix, and can be determined by inputting some corresponding positions between the thermography coordinates (the pixel coordinates) and the moving coordinates. Here, h_{11} to h_{33} parameters are determined by inputting no less than 6 corresponding points into equation (14). To allocate temperature to the 3D surface shape of an object, Equation (14) is written as follow.

$$\begin{cases} u_t = (h_{11}x_r + h_{12}y_r + h_{13}z_r + h_{14})/(h_{31}x_r + h_{32}y_r + h_{33}z_r + 1) \\ v_t = (h_{21}x_r + h_{22}y_r + h_{23}z_r + h_{24})/(h_{31}x_r + h_{32}y_r + h_{33}z_r + 1) \end{cases} \tag{15}$$

Once the calibration parameters and the moving coordinates are determined, the corresponding thermography coordinates can be calculated using equation (15), and the corresponding temperature data can be allocated to the reconstructed surface of the object.
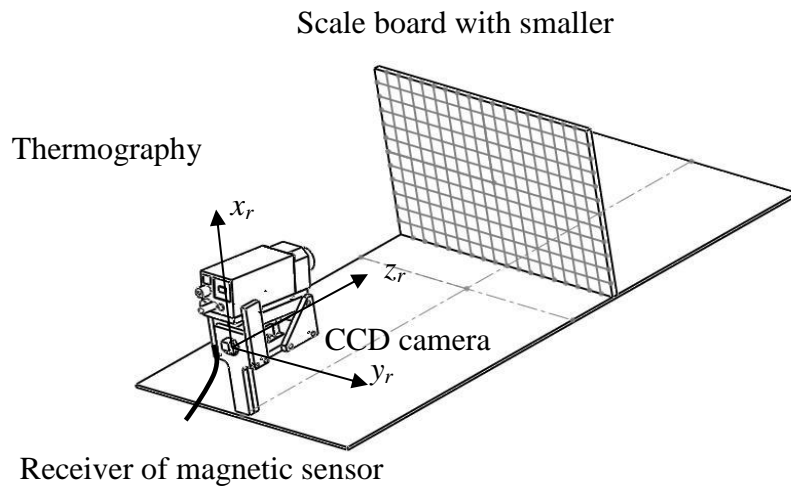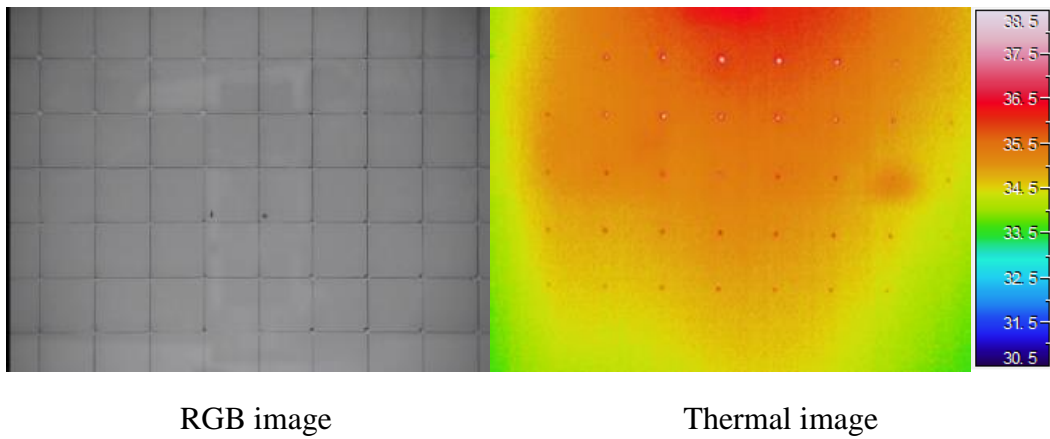
Scale board with smaller

Thermography

x_r

z_r

CCD camera

y_r

Receiver of magnetic sensor

Fig.4-4 Calibration setup

RGB image   Thermal image
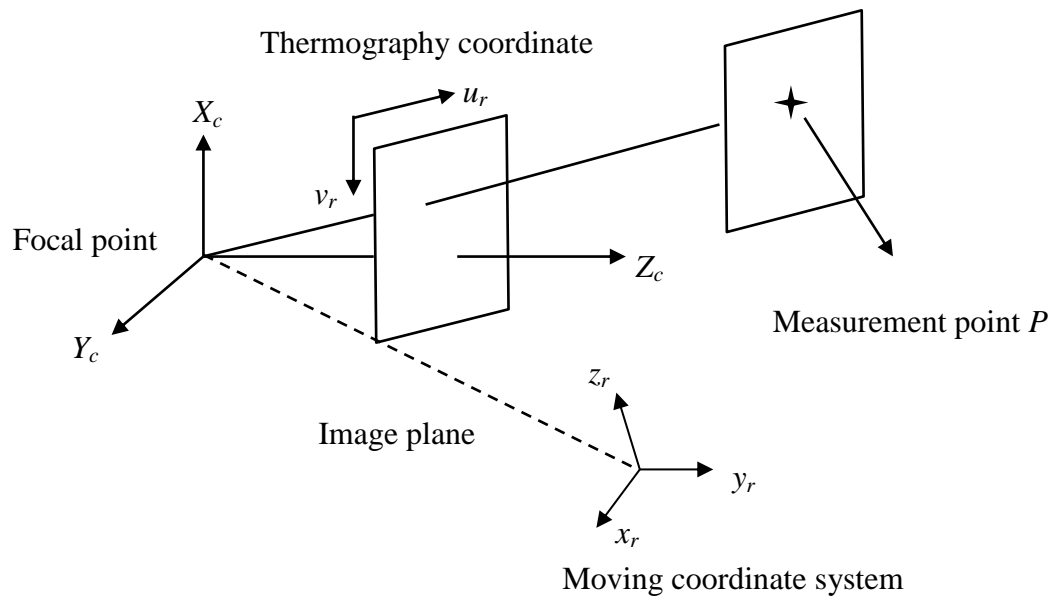
Fig. 4-5 Calibration images

Fig.4-6 Relationship between the thermography coordinate and the moving coordinate

4.5 Evaluation experiment

4.5.1 Accuracy evaluation

(1) 3D measurement device

Since the size of the object appearing in the RGB image varies depending on the distance from the CCD camera to the object, and quantitative measurement relates pixel coordinates in the RGB image, the distance from the CCD camera to the object influences the measurement accuracy. Therefore, measurement accuracy is evaluated by changing the distance from the CCD camera to the object. To verify the relation between random error and the distance from CCD camera to the object, a plane scale board is measured. Precision evaluation was executed by taking the difference between the measured value and the intrinsic dimensions at various distances from 400mm to 1300mm at 100mm intervals. The measurement accuracy for distance is shown in Fig.4-7. When the distance from the CCD camera to the object was not over 800mm, the error was less than 2mm.

In addition, since the system is based on the principle of triangulation, the angle between the CCD camera and the laser projector influences the measurement accuracy. Therefore, the angle between the CCD camera and the laser slit was changed by 5 degree, and the measurement accuracy was evaluated. Fig.4-8 shows the measurement accuracy for angle. Here, the plane scale board was set at distance 480mm. When the angle was over 40 degree, the error was less than 2mm.
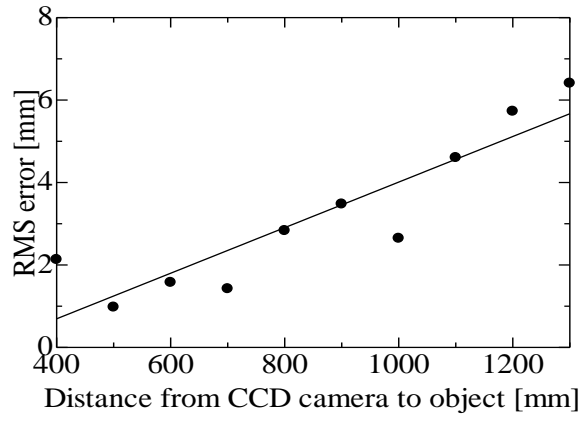
Fig.4-7 Measurement accuracy for distance
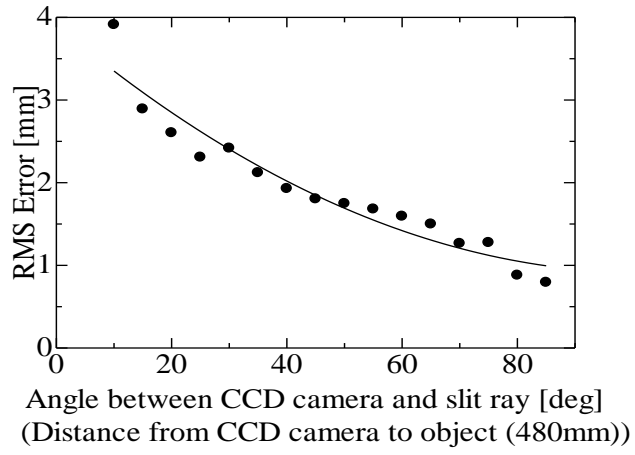

Fig.4-8 Measurement accuracy for angle

(2) Thermography

Measurement accuracy for thermography was also carried out. Since the size of the object appearing in thermal image also varies depending on the distance from the thermography to the object, the distance influences temperature allocation result. So measurement accuracy is evaluated by changing the distance from the thermography to the object. Fig.4-9 shows the measurement accuracy for temperature error considering the 3D shape. When the distance from thermography to object was not over 200cm, the error is less than 2 ^0C. On the other hand, if a cylindrical object is measured by the proposed measurement device, we can find that accuracy of temperature distribution on both sides of the cylindrical object will come down. For example, Fig.4-10 shows thermal image of a can. Fig.4-11 shows the temperature distribution. By the experiment result, due to the dependence of the emissivity on the viewing angle, the shape of the surface affects the results of infrared measurement. A cardboard is used for accuracy evaluation and measurement accuracy is evaluated by ranging from -90° to 90° as Fig.4-12.
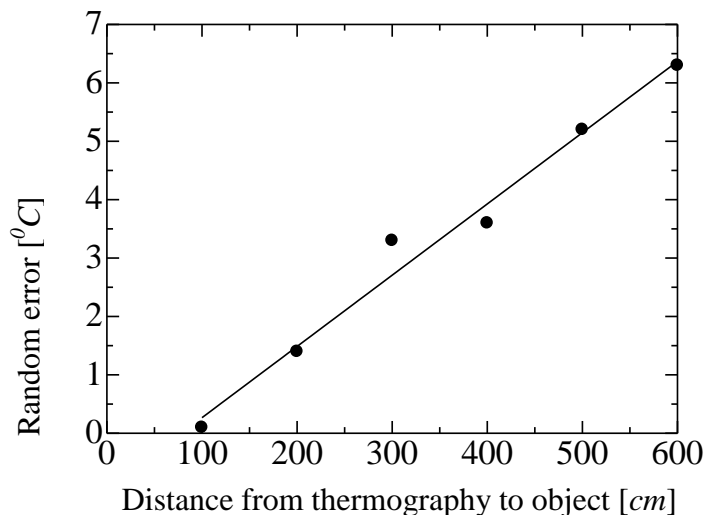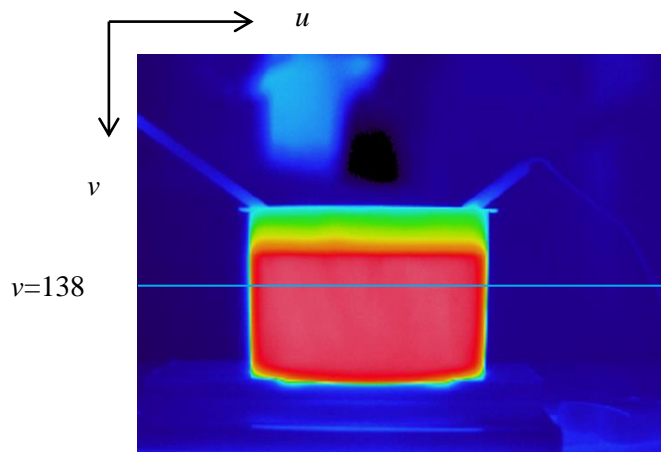

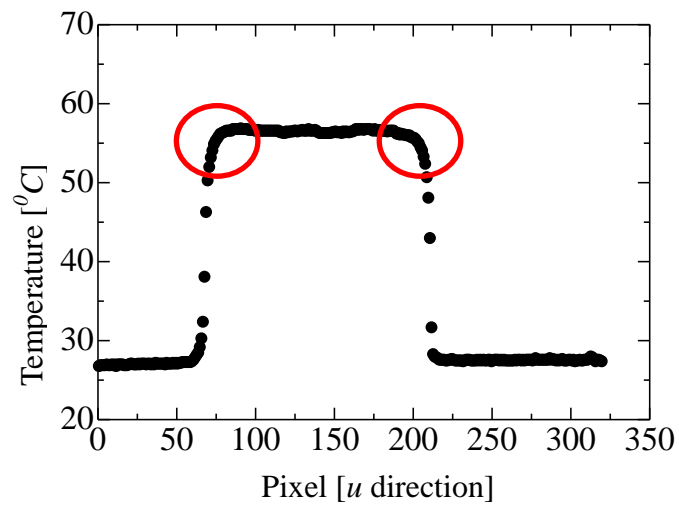**Fig.4-9** Measurement accuracy

Fig.4-10 Thermal image
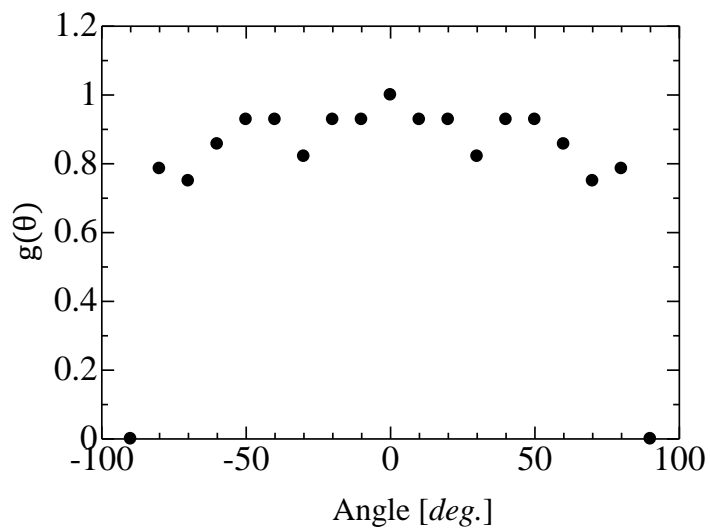

Fig.4-11 Temperature distribution (*v*=138)

Fig.4-12 Measurement accuracy

In Fig.4-12, the expression $g(\theta) = \frac{T_{IR}(\theta) - T_{amb}}{T_{IR}(\theta=90°) - T_{amb}}$ is plotted versus angle θ, where T_{amb} indicates the ambient temperature. This plot indicates a nearly constant emissivity for an angle between 0° to 60°. When angle is higher than 60°, the emissivity is decreased and so reliable infrared measurements are no more possible.

4.5.2 Measurement result

In this Chapter, measurement result of a resin part is introduced for one of the examples of the 3D temperature measurement in industry filed. Fig.4-13 shows the measurement result. In addition, the measurement result of a human hand is introduced for one of the examples of the 3D temperature measurement in medical filed. The 2D thermal-image is shown in Fig.4-14, and the 3D temperature distribution of a human hand is shown in Fig.4-15. By the experiment results, since 3D temperature distribution of an object can be obtained easily using our system, the proposed system is expected to be a useful tool in biological field.
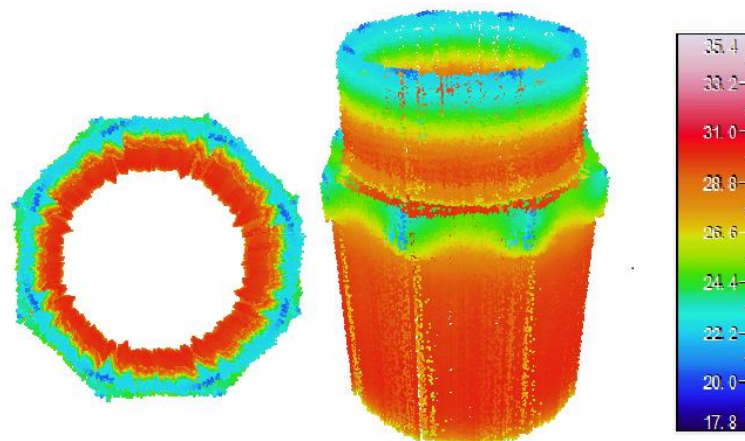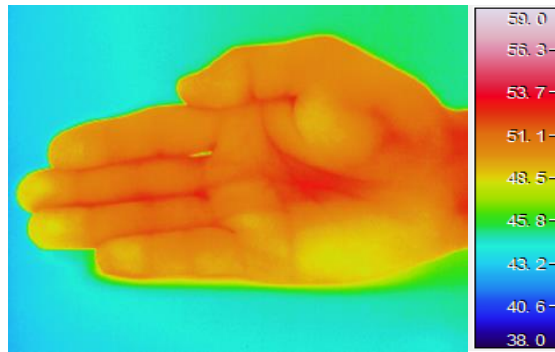

Fig.4-13 Measurement result
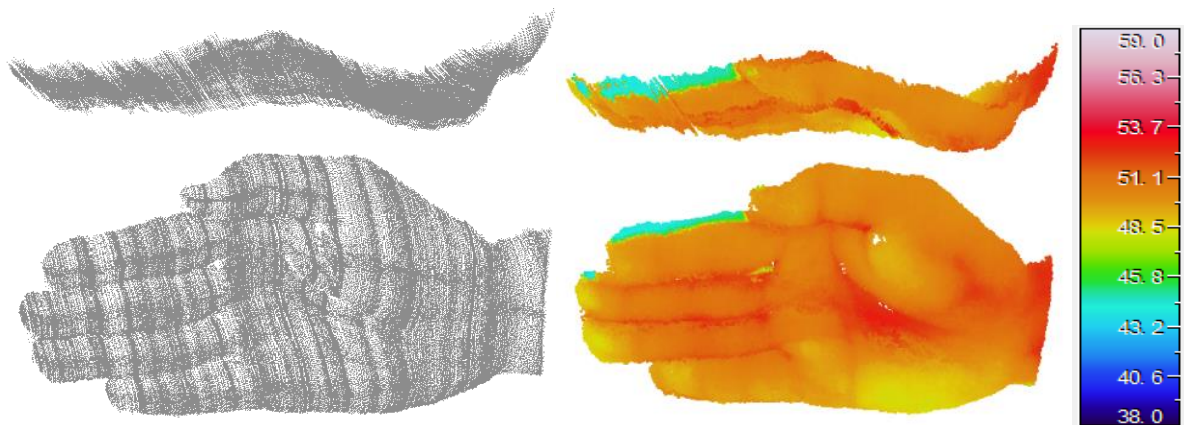
Fig.4-14 Calibration images

Fig.4-15 3D temperature distribution of a human hand

4.6 Conclusion

In this Chapter, a system which is established by combining a light-section method and a magnetic sensor was introduced. Since the laser-projection unit and the image-capture unit (i.e., the CCD camera and the thermography device) can be moved freely by mounting magnetic sensors on them, the proposed system can easily measure 3D temperature distribution of an object regardless of the shape and the size of an object. In addition, since image-capture unit image-capture unit can be moved freely, occlusion problem can be solved.

On the basis of the presented mathematical model, since this system can detect not only the three-dimensional shape but also the temperature distribution of an object simultaneously, it can be utilized for the analysis of heat radiation in various fields. In addition, since 3D thermograms can be registered accurately, comparisons and analyses can be performed using image processing techniques.

CHAPTER 5: Conclusion

Three-dimensional thermo-sensing systems using a computer vision are introduced in the present dissertation. Based on the proposed mathematical model, the systems can detect not only the 3D shape of an object, but also its temperature distribution. The experimental results of the present study demonstrated the feasibility of the proposed systems. The construction of the proposed system and an analysis algorithm were described, and the validity of the proposed systems was verified. The primary conclusions of the present dissertation are as follows.

In Chapter 2, a method of representing 3D thermal images was introduced. A conceptual model of a 3D thermography that introduces 3D thermogram creation, representation, and analysis concepts that are useful for a variety of medical and industrial applications was proposed. The creation of a 3D thermogram is possible by combining 3D measurement methods with thermal images captured by the thermography device. The present dissertation described the development of a 3D thermo-sensing system that integrates passive thermal imaging with 3D geometrical data obtained from an active 3D measurement instrument.

In Chapter 3, an investigation of the geometric quality of 3D data obtained by the new thermal-sensing system was presented. The measurement system is composed of a portable 3D measurement instrument (Kinect sensor) and an infrared thermography device. Since the Kinect sensor can measure the 3D shape of an object instantaneously, the measurement time is significantly reduced. In addition, when the instrument is moved, the system can measure the entire perimeter of a target object by automatically splicing the obtained shape data using the iterative closest point (ICP) algorithm.

In Chapter 4, a system that can be used to measure the 3D shape of an object by maintaining the proper angle between the laser-projection unit and the image-capture unit was proposed. The laser-projection unit and the image-capture unit are made independent of each other by mounting 3D magnetic sensors on them. Since the movement of the image-capture devices is detected in

real-time by the magnetic sensors, areas that cannot be measured can be reduced. Thus, using the

proposed system, a 3D thermogram can be obtained regardless of the size of the measurement

object.

References

[1] T. Sakagami, "Thermoelastic Stress Measurement by Infrared Thermography (Serial Lecture Paper2)", *Japan Welding Society*, Vol.72(6) (2003),pp.511-515

[2] T. Sakagami, S. Kubo, et al, "Identification of plastic zone based on temperature distribution measured by infrared thermography", *The Japan Society of Mechanical Engineers*, pp.217-218 (2008)

[3] H. Ando, C. Kobayashi, et al, "Heating Condition of Active Infrared Thermography for Concrete Structures", *The Japan Society of Mechanical Engineers*, pp. 4-5 (2010)

[4] K. Kawasue,N. Taguchi, "Three-dimensional Measurement Using Silhouette Images From Random Angles", *The japan Society of Mechanical Engineers C*,Vo.71,No.04-0832 (2005),pp.115-121

[5] K. Kawasue, S. Aramaki, "Hybrid Measurement System For Fluid And Solid", *The Japan Society of Mechanical Engineers*, J24(2006(59)),pp. 269-270

[6] K. Kawasue, H. Ngagatomo, H. Shiraishi, "Measurement of Agricultural Products Using Silhouette Images from Random Angles", *The Japan Society of Mechanical Engineers*,J23 (2006(59)),pp.269-268

[7] K. Kawasue, G. Uezono, el al., "Three-dimensional Measurement by Free Scanning of a CCD camera and Laser", *WSEAS transactions on System*,(2004),1(Vol.3),pp.143-147

[8] Y. Oya, K. Kawasue, "Three Dimensional Measurement of fish movement using stereo vision", *International Journal of Artificial Life and Robotics*,(2008),Vol.13pp.69-72

[9] M. Ikeda, "High Speed 3D Range Capture Techniques", *The Institute of Information and Television Engineers*, *ITE Technical Report* Vol.34,No.16 (2010),pp. 9-14

[10] K. Hattori, el al., "Hardware design for Real-time 3D Mesh Generation", *The Institute of Image Information and Television Engineers*, *ITE Technical Report* ,Vol.34,No.43 (2010), pp.57-60

[11] Y. Oike, M. Ikeda, K. Asada, "640×480 Real-Time Range Finder Based on Light-Section Method", *The Institute of Image Information and Television Engineers*, *ITE Technical Report*, Vol.27, No.25 (2003), pp.1-4

[12] K. Yamauchi, S. Shibata, and Y. Sato, "Three-Dimensional Human Body Measurement Using Multiple Range Image", *The Institute of Electronics, Information and Communication Engineers*, Vol.J88-D-II, No.8(2005), pp.1564-1572

[13] A. Nakano, D. Nakayama, el al., "Stereoscopic 3-D Measurement of Objects in a Glass Water Tank", *Institute of Electronics, Information, and Communication Engineers*, pp.1-6 (2000)

[14] K. Matsubara, Y. Sasamoto, el al., "Research on 3D shape measurement by stereo method", *The Japan Society of Mechanical Engineers*, pp.27-28 (2008)

[15] A. Zontak, S. Sideman, el al., "dynamic Thermography: Analysis of Hand Temperature During Exercise", *Annals of Biomedical Engineering*, Vol.26, pp.9988-993 (1998)

[16] Barnes, R.B, "Thermography", *Ann. N.Y. Acad. Sci.*, Vol.121, pp.34-48 (1964)

[17] R.Y. Tsai, A Versatile Camera Calibration Technique for High-Accuracy 3D Machine Vision Metrology Using Off-the-Shelf TV Cameras and Lenses, *IEEE Journal of Robotics and Automation*, Vol. RA-3, pp. 323-344 (1987)

[18] T. Ueshiba and F. Tomita, Calibration of Multi-camera Systems Using Planar Patterns, *Information Processing Society of Japan*, vol. 44, pp. 89–99 (2003)

[19] K. Miyazaki, el al., "Calibration Technique of PIV for Distorted Image Using LCD", *IEEE International Symposium on Industrial Electronics*, pp.301-306 (2009)

[20] S. Watanabe, Y. Yamanaka, el al., "An Exposure Setup for In Vivo Studies to Test Biological Effects in a Head Locally Exposed to MW from a Cellular Telephone", *Institute of Electronics, Information, and Communication Engineers*,pp.15-22 (1998)

[21] H. Nagahara, and Y. Ebina, "Extraction of characteristic features in individual human faces from thermal distribution images", *Institute of Electronics, Information, and Communication*

Engineers, pp.39-44

[22] J. R. Speakman and S. Ward, "Infrared thermography: principles and applications", *ZOOLOGY Analysis of Complex Systems*, pp.224-232 (1998)

[23] J. Christensen, el al., "Thermography as a quantitative imaging method for assessing postoperative inflammation ", *DentoMaxilloFacial Radiology* (2012)41, pp.494-499

[24] X. Ju, J.C. Nebel, and J.P. Sieber, "3D Thermography Imaging Standardization Technique for Inflammation Diagnosis", *Proc. Of SPIE*, pp.5640-5646 (2004)

[25] H. Fujita, H. Kano, el al., "hand-held 3D Scanner Using Two-stage Active Stereo Method", *The Institute of System, Control and Information Engineers*, Vol.15, No.4, pp.213-219 (2002)

[26] J. Smisek, M. Jancosek and T. Pajdla, "3D with Kinect", *CDC4CV*, pp. 1154-1160 (2011)

[27] L. Xia, C.C. Chen, and J.K. Aggarwal, "Human Detection Using Depth Information by Kinect", pp.15-22 (2011)

[28] Z.Y. Zhang, "Microsoft Kinect Sensor and Its Effect", pp. 4-10 (2012)

[29] K. Lai, L. Bo, X. Ren and D. Fox, "A Large-Scale Hierarchical Multi-View RGB-D Object Dataset", *ICRA*. (2011)

[30] S. Rusinkiewicz and M. Levoy, "Efficient Variants of the ICP Algorithm", *In proceedings of the International Conference on 3D Digital Imaging and Modeling (3DIM)*, pp.145-152 (2001)

[31] A.E. Johnson and S.B. Kang, "Registration and Integration of Textured 3-D Data", *Image and Vision Computing*, Vol.17, pp.135-147 (1999)

[32] K. Matsui, A. Yamashita and T. kaneko, "3-D Shape Reconstruction of Pipe with Omni-Directional Laser and Omni-Directional Camera", *Asian Symposium for Precision Engineering and Nanotechnology* (2009)

[33] 徐　剛, 辻　三郎：三次元ビジョン，共立出版 (1998)

[34] E.R. Davies, Machine Vision: Theory algorithms, Practicalities, Academic press (1990)

[35] Carme Torras, "Computer Vision: Theory and Industrial Applications", Springer-Verlag (1992)

[36] D.H. Qin, J.J. Liu, T. Mao, "Handheld Laser Scanning 3-D Profilometry System for Rock Based on Binocular Stereo Vision", *Physical and Numerical Simulation of Geotechnical Engineering 2nd ISSUE*, pp.111-114 (2011)

Acknowledgement

I would like to express my deepest and sincerest gratitude to my supervisor, Professor, Ph.D. Kikuhito Kawasue, Faculty of Engineering, University of Miyazaki, for providing excellent supervision, valuable insight, and encouragement in my research. His productive comments and advice was a major guidance during my study period. He has taught me, both consciously and un-consciously, how good experimental is done. His enthusiasm for research was contagious and motivational for me.

I also would like to thank to my advisor, Professor Dr. Koichi Tanno and Associate Professor Hiroki Tamura, Faculty of Engineering, University of Miyazaki, for providing precious opinion to improve the quality of my paper. And, I would like to express many of my thanks to Dr. Koji Miyazaki for his advice during creating paper and thanks to Shigeki Ohyama for his advice during making programs.

I am highly indebted to everybody of the staffs in laboratory, University of Miyazaki, Faculty of Engineering, Measurement and Control Laboratory during my research. The members of laboratory have contributed immensely to my personal and professional time. Our research group has been a source of friendships as well as good advice and collaboration. I think that it is the best group in our school.

Many thanks for help of Satoshi Nagatomo, who is a staff of Miyazaki University Education Research Support Technology Center during the measuring device manufacturing.

Lastly, I would like to thank my family for all their love and encouragement. And, for my parents who raised me with a love of science and supported me in all my pursuits.

Tao Li

University of Miyazaki

March 2014

66